The Multiple Scales of El Niño

Cécile Penland

NOAA/ESRL/Physical Sciences Division

With thanks to P.D. Sardeshmukh, L. Matrosova, G. Compo, M. Newman, P.Sura and a cast of dozens.

Outline

- Climatology (What's normal?)
- Basic properties of El Niño
- Linear Inverse Modeling
- Non-normal growth and the optimal structure
- Short scales: What constitutes stochastic forcing?
- Long scales: Connection between El Niño and the Pacific Decadal Oscillation

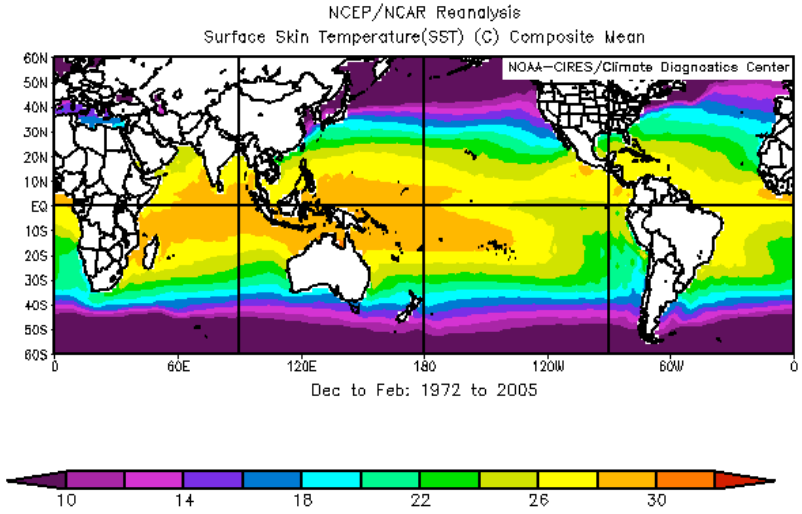
NCEP/NCAR Reanalysis
Surface Skin Temperature(SST) (C) Composite Mean
NOAA–CIRES/Climate Diagnostics Center
60N
50N
40N
30N
20N
10N
EQ
10S
20S
30S
40S
50S
60S
0
60E
120E
180
120W
60W
0
Dec to Feb: 1972 to 2005
10
14
18
22
26
30

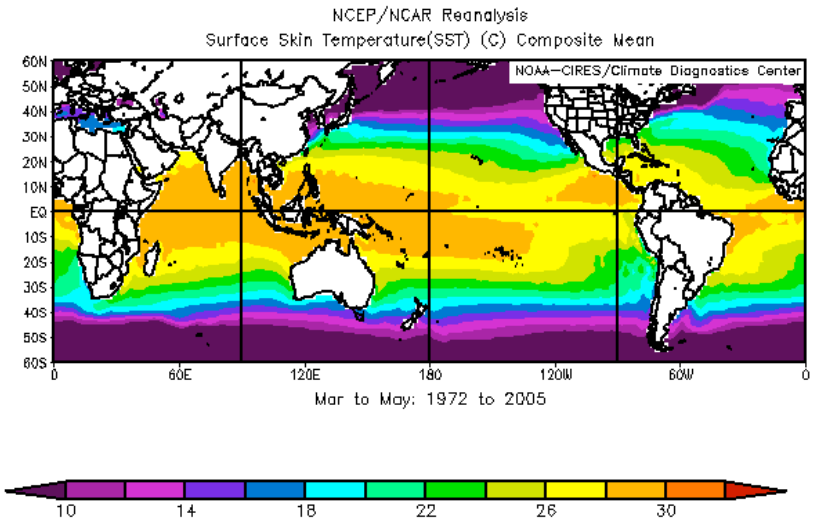
NCEP/NCAR Reanalysis
Surface Skin Temperature(SST) (C) Composite Mean
NOAA–CIRES/Climate Diagnostics Center
60N
50N
40N
30N
20N
10N
EQ
10S
20S
30S
40S
50S
60S
0
60E
120E
180
120W
60W
0
Mar to May: 1972 to 2005
10
14
18
22
26
30

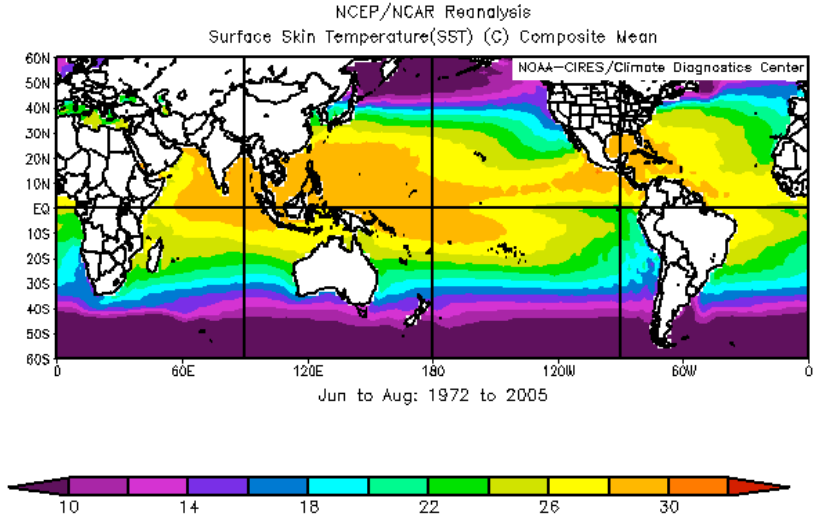
NCEP/NCAR Reanalysis
Surface Skin Temperature(SST) (C) Composite Mean
NOAA–CIRES/Climate Diagnostics Center
60N
50N
40N
30N
20N
10N
EQ
10S
20S
30S
40S
50S
60S
0
60E
120E
180
120W
60W
0
Jun to Aug: 1972 to 2005
10
14
18
22
26
30

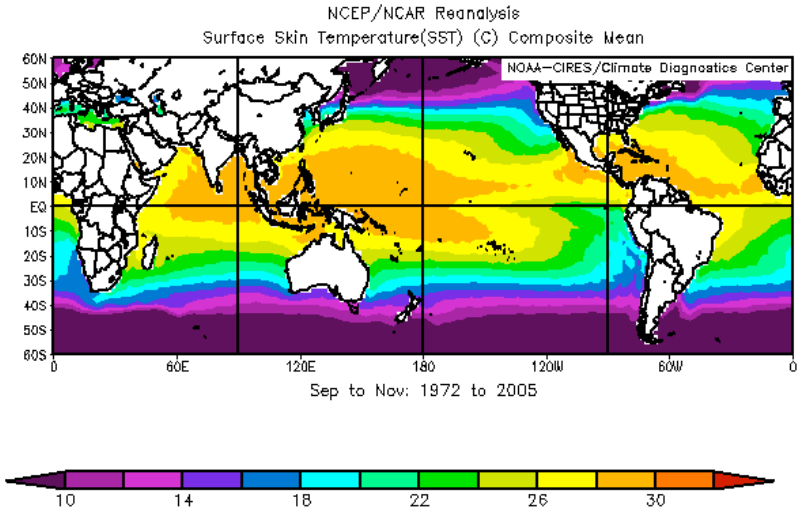
NCEP/NCAR Reanalysis
Surface Skin Temperature(SST) (C) Composite Mean
NOAA–CIRES/Climate Diagnostics Center
60N
50N
40N
30N
20N
10N
EQ
10S
20S
30S
40S
50S
60S
0
60E
120E
180
120W
60W
0
Sep to Nov: 1972 to 2005
10
14
18
22
26
30

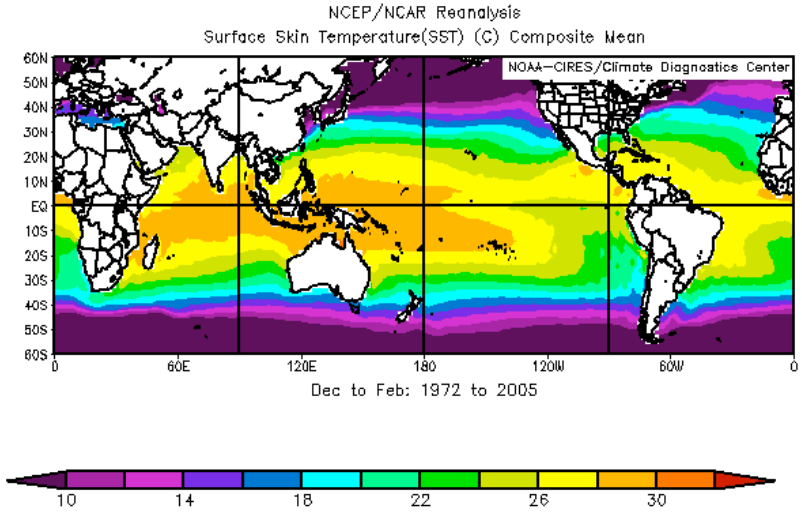
NCEP/NCAR Reanalysis
Surface Skin Temperature(SST) (C) Composite Mean
NOAA–CIRES/Climate Diagnostics Center
60N
50N
40N
30N
20N
10N
EQ
10S
20S
30S
40S
50S
60S
0
60E
120E
180
120W
60W
0
Dec to Feb: 1972 to 2005
10
14
18
22
26
30

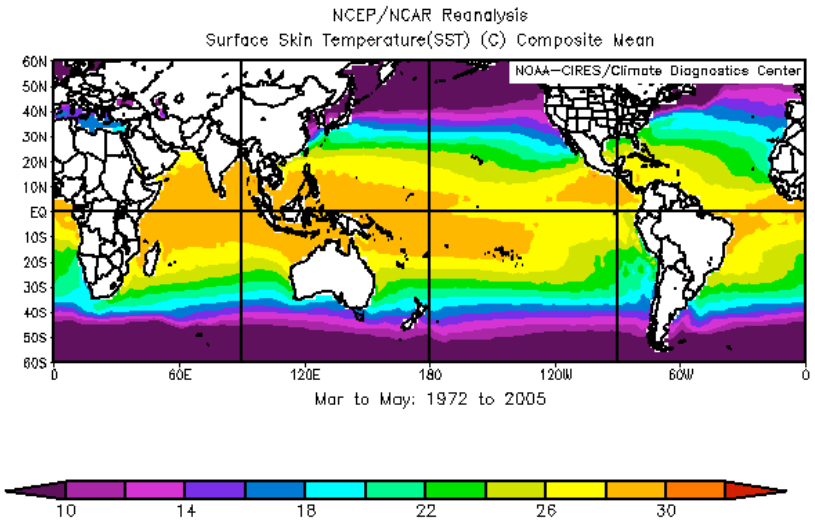
NCEP/NCAR Reanalysis
Surface Skin Temperature(SST) (C) Composite Mean
NOAA–CIRES/Climate Diagnostics Center
60N
50N
40N
30N
20N
10N
EQ
10S
20S
30S
40S
50S
60S
0
60E
120E
180
120W
60W
0
Mar to May: 1972 to 2005
10
14
18
22
26
30

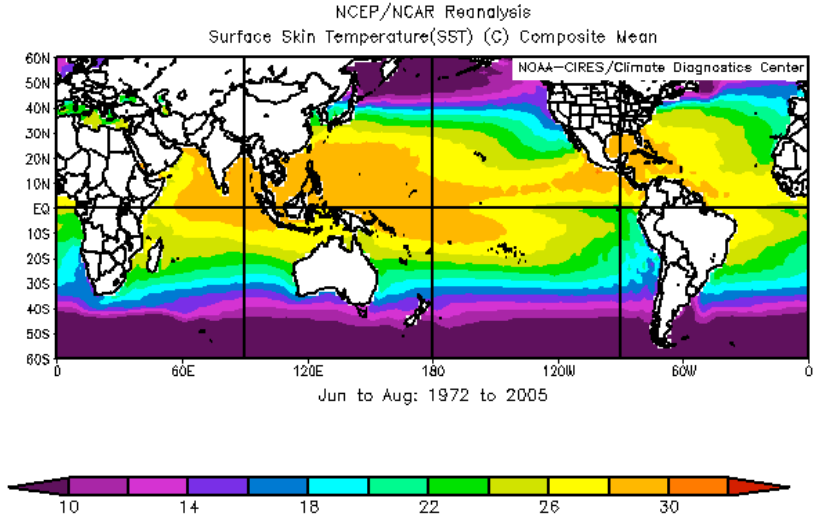
NCEP/NCAR Reanalysis
Surface Skin Temperature(SST) (C) Composite Mean
NOAA–CIRES/Climate Diagnostics Center
60N
50N
40N
30N
20N
10N
EQ
10S
20S
30S
40S
50S
60S
0
60E
120E
180
120W
60W
0
Jun to Aug: 1972 to 2005
10
14
18
22
26
30

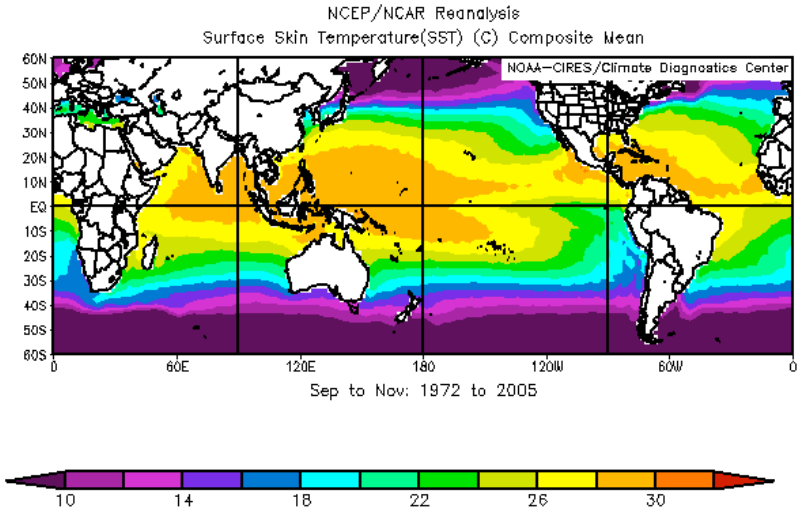
NCEP/NCAR Reanalysis
Surface Skin Temperature(SST) (C) Composite Mean
NOAA–CIRES/Climate Diagnostics Center
60N
50N
40N
30N
20N
10N
EQ
10S
20S
30S
40S
50S
60S
0
60E
120E
180
120W
60W
0
Sep to Nov: 1972 to 2005
10
14
18
22
26
30

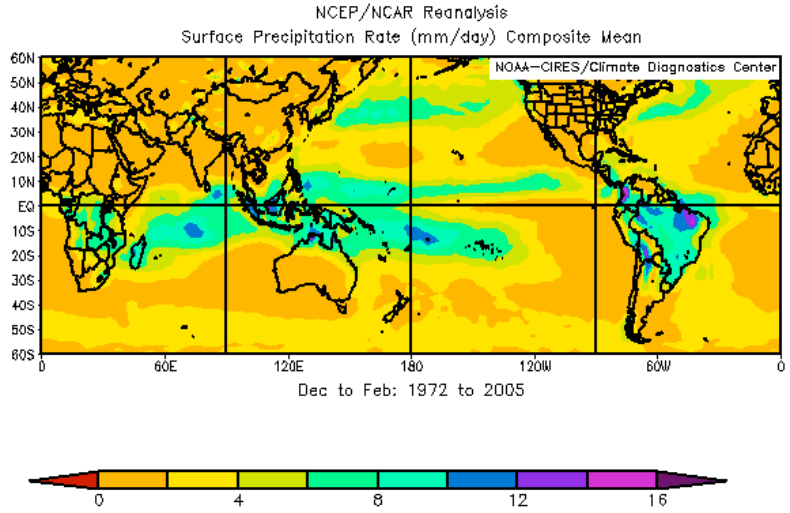
NCEP/NCAR Reanalysis
Surface Precipitation Rate (mm/day) Composite Mean
NOAA–CIRES/Climate Diagnostics Center
60N
50N
40N
30N
20N
10N
EQ
10S
20S
30S
40S
50S
60S
0
60E
120E
180
120W
60W
0
Dec to Feb: 1972 to 2005
0
4
8
12
16

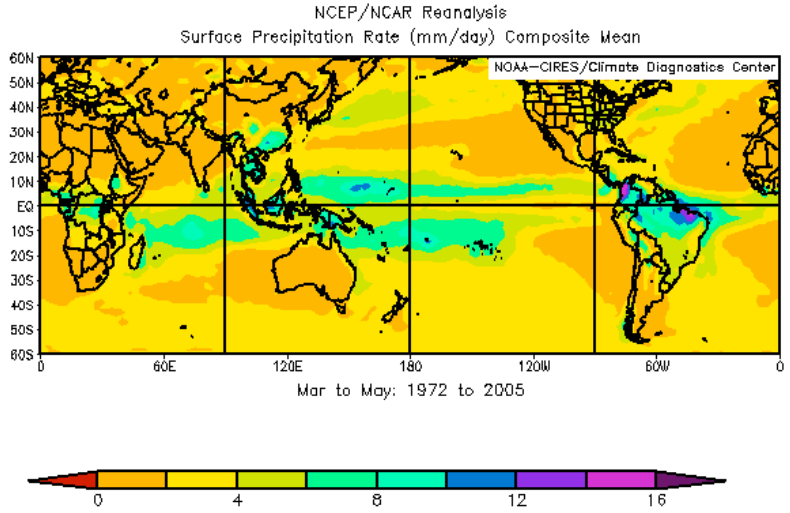
NCEP/NCAR Reanalysis
Surface Precipitation Rate (mm/day) Composite Mean
NOAA–CIRES/Climate Diagnostics Center
60N
50N
40N
30N
20N
10N
EQ
10S
20S
30S
40S
50S
60S
0
60E
120E
180
120W
60W
0
Mar to May: 1972 to 2005
0
4
8
12
16

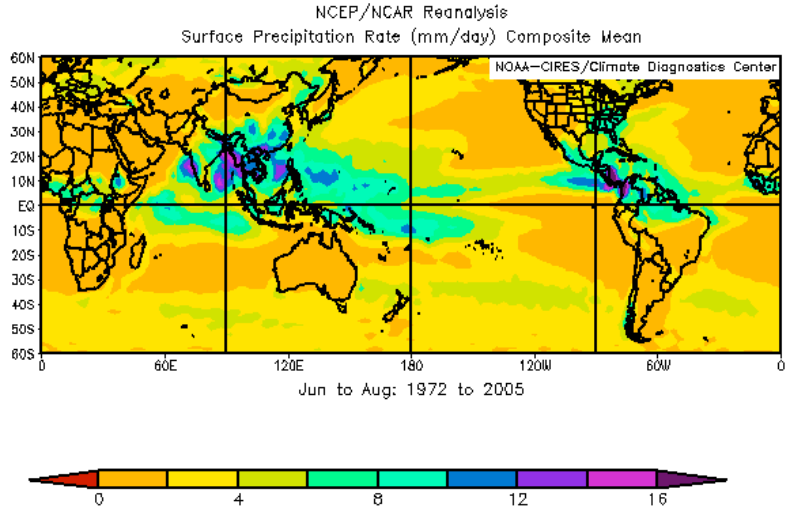
NCEP/NCAR Reanalysis
Surface Precipitation Rate (mm/day) Composite Mean
NOAA–CIRES/Climate Diagnostics Center
60N
50N
40N
30N
20N
10N
EQ
10S
20S
30S
40S
50S
60S
0
60E
120E
180
120W
60W
0
Jun to Aug: 1972 to 2005
0
4
8
12
16

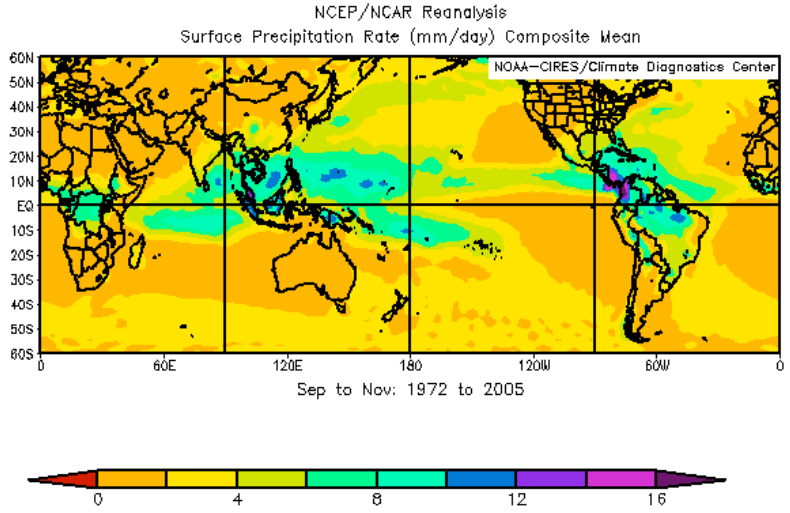
NCEP/NCAR Reanalysis
Surface Precipitation Rate (mm/day) Composite Mean
NOAA–CIRES/Climate Diagnostics Center
60N
50N
40N
30N
20N
10N
EQ
10S
20S
30S
40S
50S
60S
0
60E
120E
180
120W
60W
0
Sep to Nov: 1972 to 2005
0
4
8
12
16

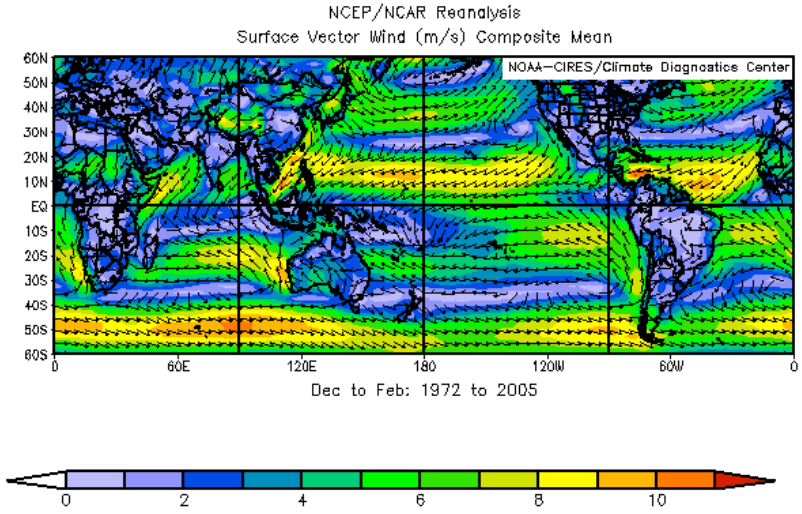
NCEP/NCAR Reanalysis
Surface Vector Wind (m/s) Composite Mean
NOAA–CIRES/Climate Diagnostics Center
60N
50N
40N
30N
20N
10N
EQ
10S
20S
30S
40S
50S
60S
0
60E
120E
180
120W
60W
0
Dec to Feb: 1972 to 2005
0
2
4
6
8
10

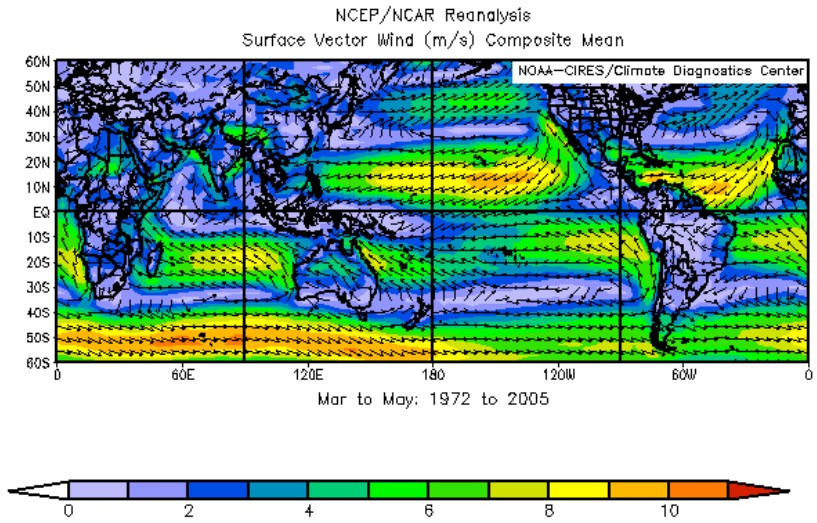
NCEP/NCAR Reanalysis
Surface Vector Wind (m/s) Composite Mean
NOAA–CIRES/Climate Diagnostics Center
60N
50N
40N
30N
20N
10N
EQ
10S
20S
30S
40S
50S
60S
0
60E
120E
180
120W
60W
0
Mar to May: 1972 to 2005
0
2
4
6
8
10

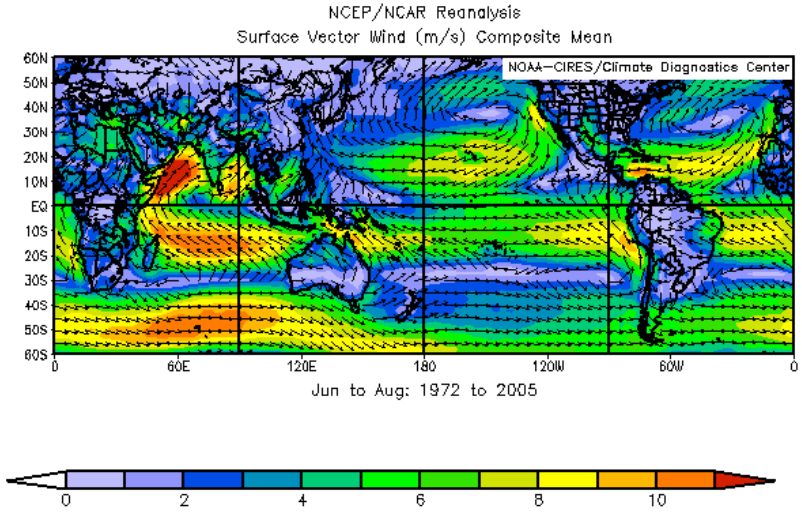
NCEP/NCAR Reanalysis
Surface Vector Wind (m/s) Composite Mean
NOAA–CIRES/Climate Diagnostics Center
60N
50N
40N
30N
20N
10N
EQ
10S
20S
30S
40S
50S
60S
0
60E
120E
180
120W
60W
0
Jun to Aug: 1972 to 2005
0
2
4
6
8
10

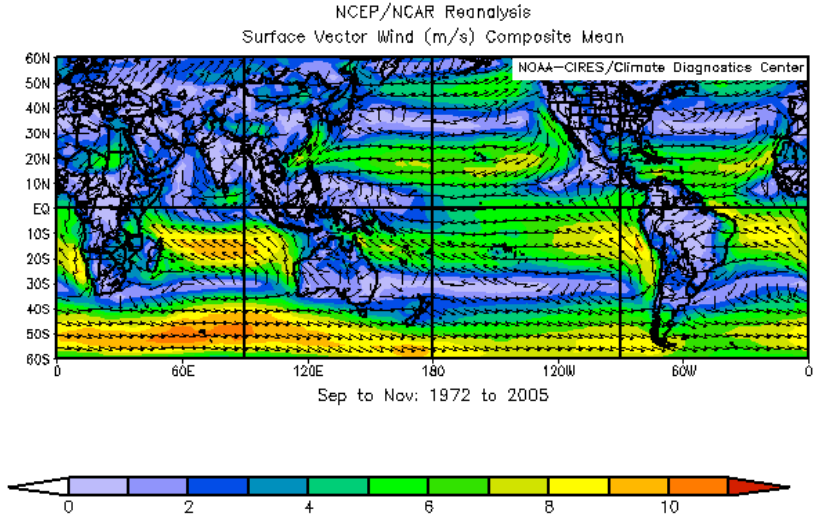
NCEP/NCAR Reanalysis
Surface Vector Wind (m/s) Composite Mean
NOAA–CIRES/Climate Diagnostics Center
60N
50N
40N
30N
20N
10N
EQ
10S
20S
30S
40S
50S
60S
0
60E
120E
180
120W
60W
0
Sep to Nov: 1972 to 2005
0
2
4
6
8
10

Rasmussen and Carpenter (1982)

FIG. 17. Antecedent conditions anomaly composite (averages for August–October of the year preceding El Niño). (a) SST (°C), (b) wind anomaly (m s^{-1}), (c) velocity divergence (10^{-6} s^{-1}). The normal positions of the axes of convergence associated with the SPCZ and ITCZ are indicated on the convergence composite. Areas in which the number of observations averages less than 10 in a two-degree square are shaded on the wind composite.

Antecendent phase (ASO -1)

Onset phase (NDJ -1)

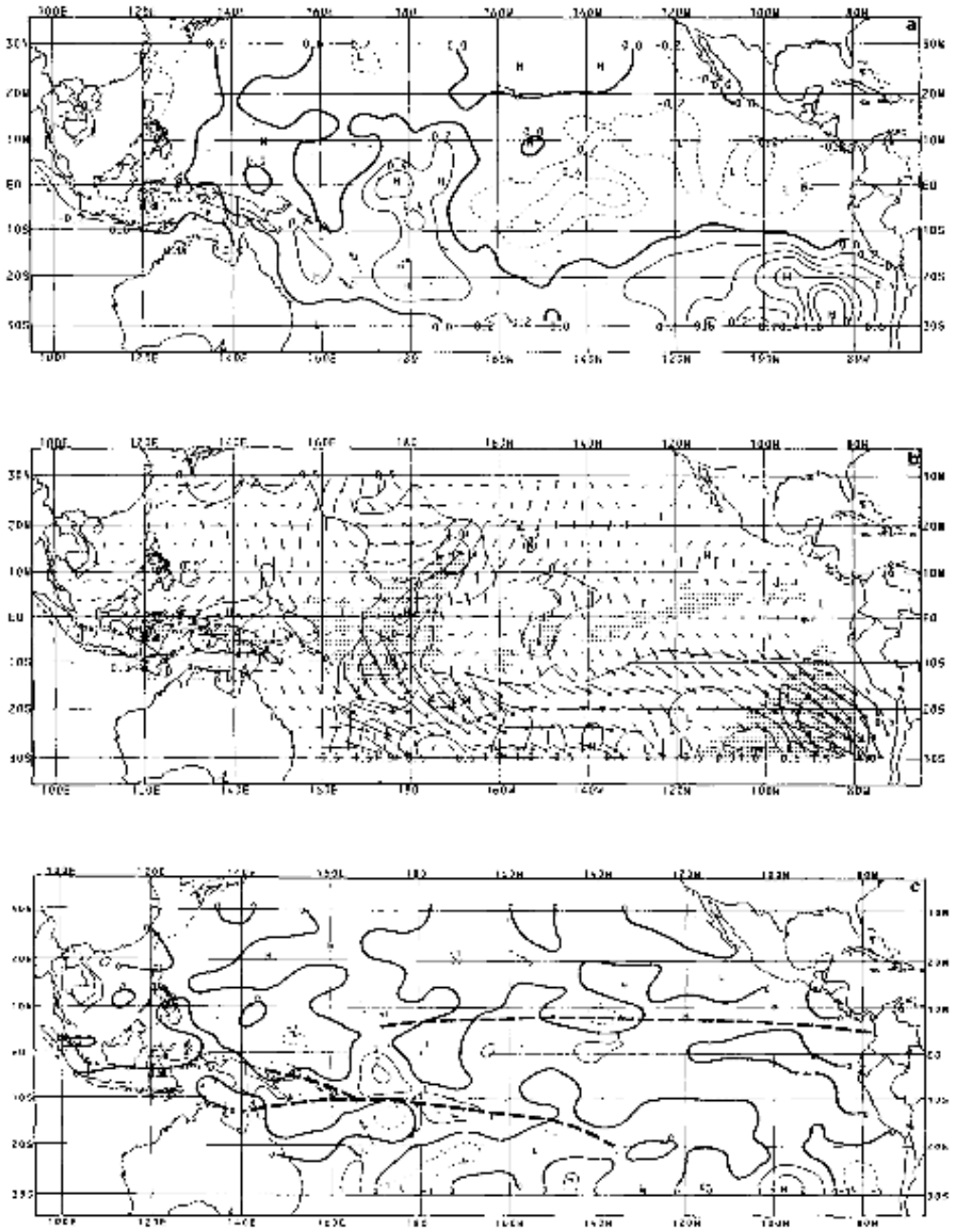

FIG. 18. Onset Phase anomaly composite. (Averages for November–January prior to maximum positive SST anomalies off Ecuador–Peru coast (Dots and shading areas as in Fig. 17.

(MAM 0)

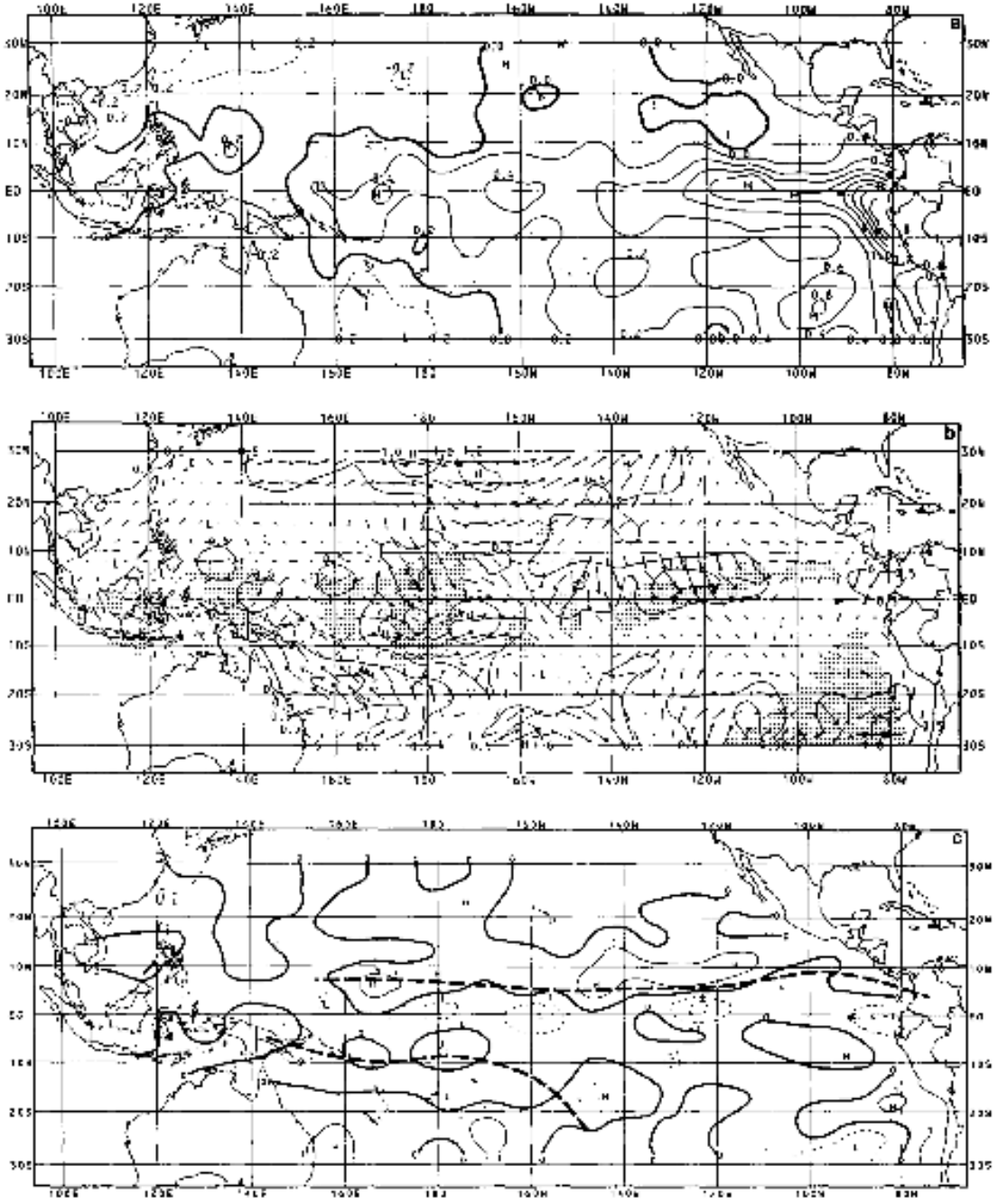

FIG. 19. Peak Phase composite. (Averages for March–May of El Niño year.) Units and shading are as in Fig. 17.

(ASO 0)

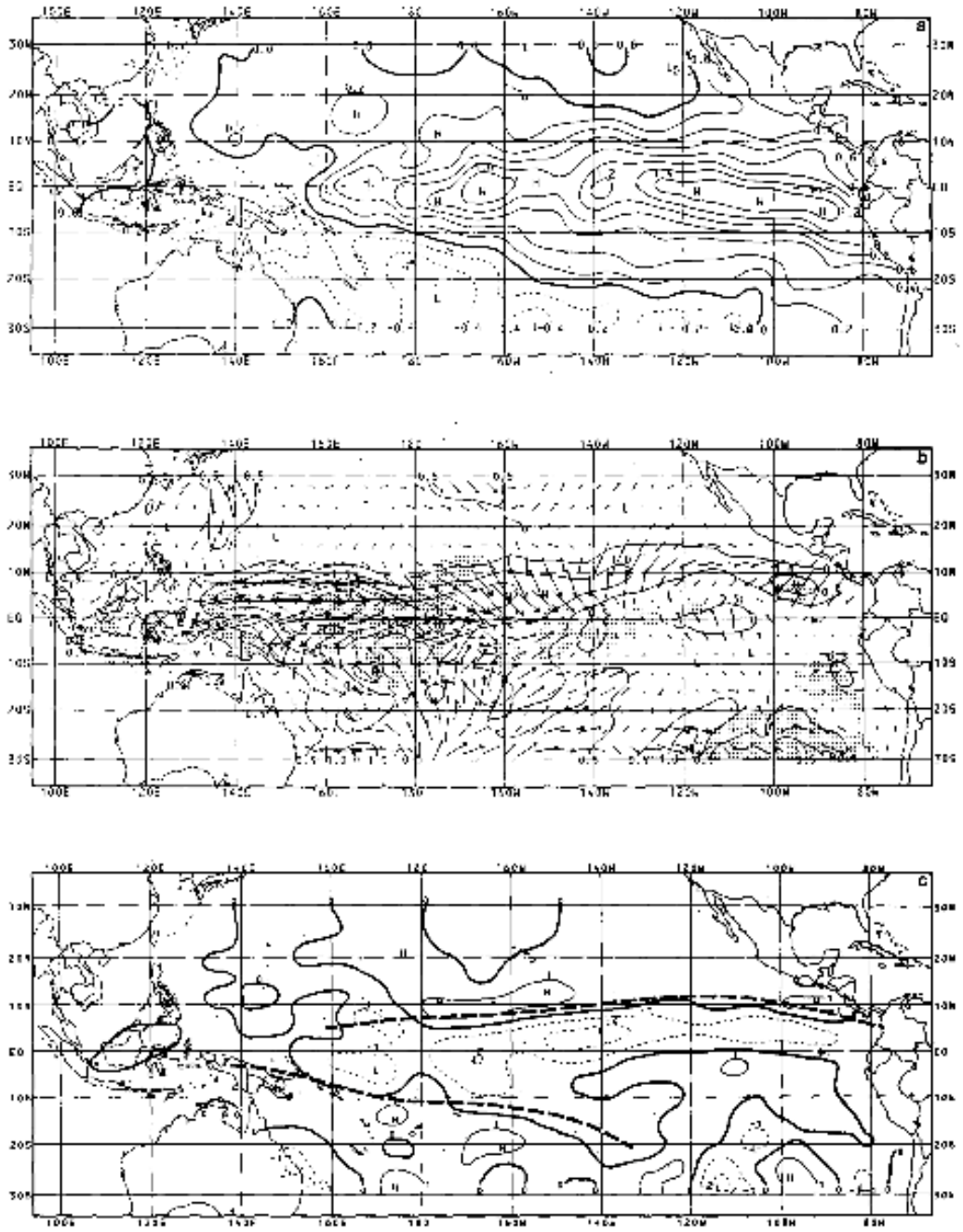

FIG. 20. Transition Phase anomaly composite (Averages for August–October of El Niño year). Units and shading are as in Fig. 17.

Mature phase
(NDJF 0)

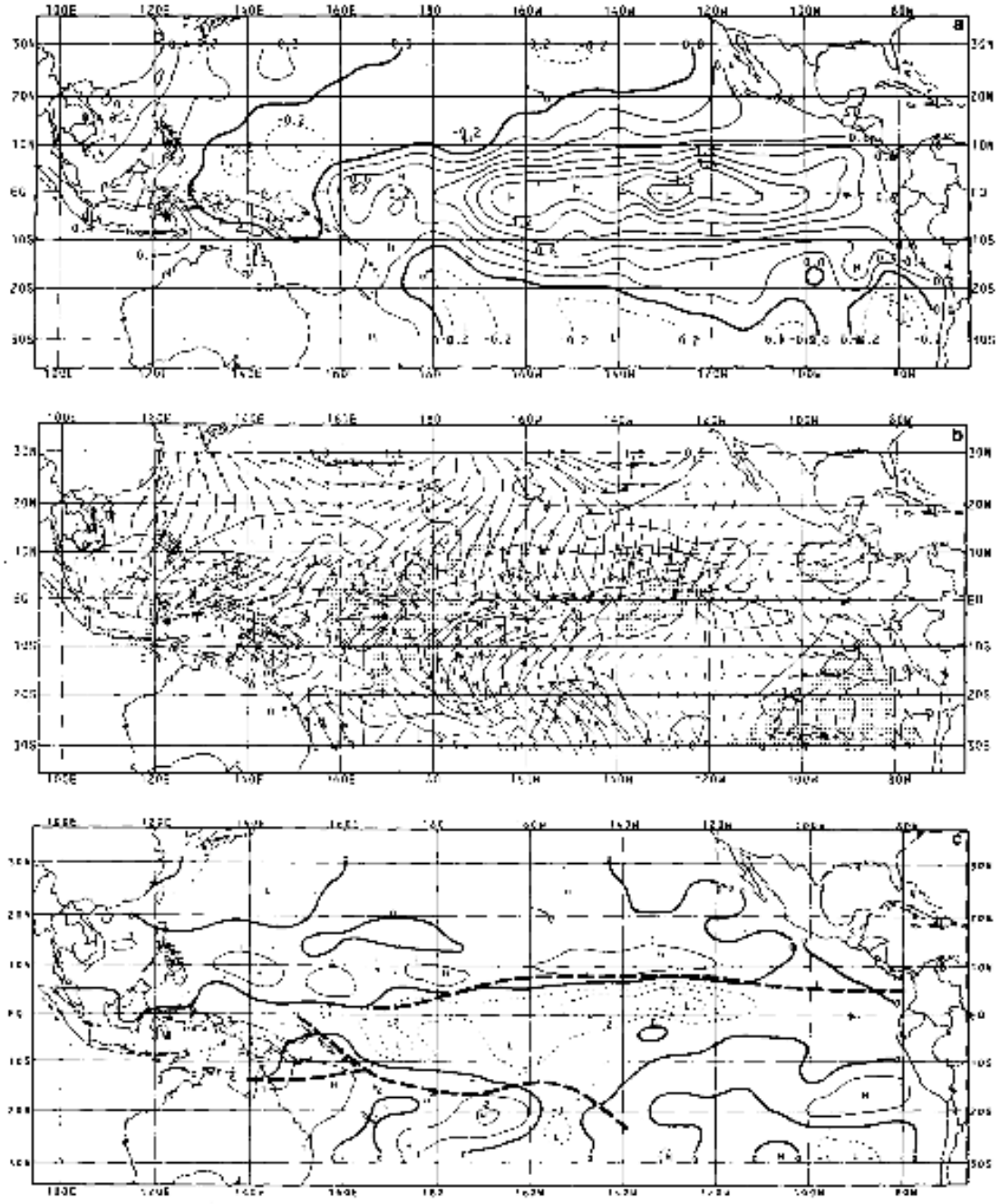

FIG. 21. Mature Phase anomaly composite. (Averages for December–February following El Niño.) Units as in Fig. 17.

Normal Conditions

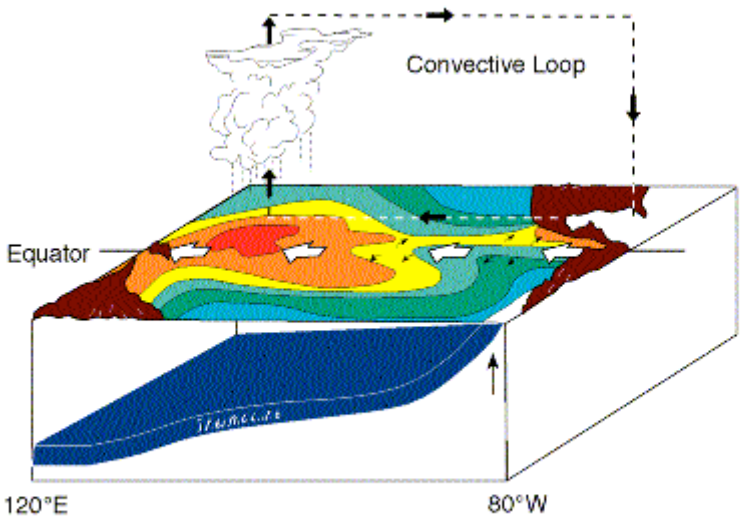

El Niño Conditions

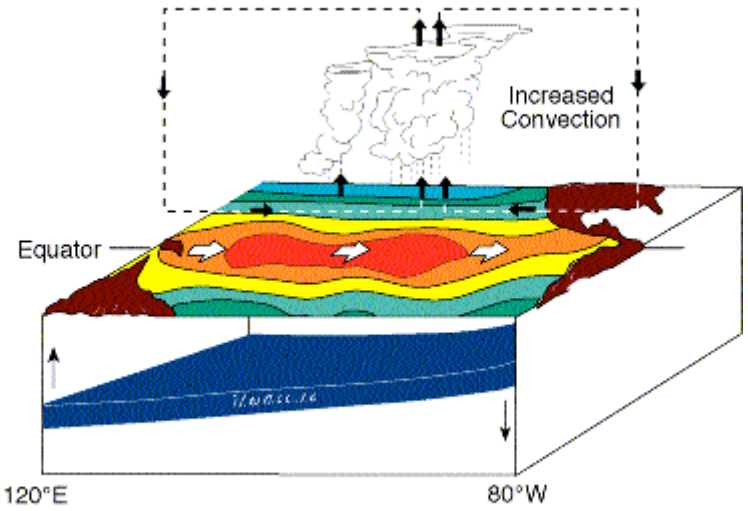

NOAA/PMEL/TAO

Five Day Zonal Wind, SST, and 20°C Isotherm Depth Anomalies 2°S to 2°N Average

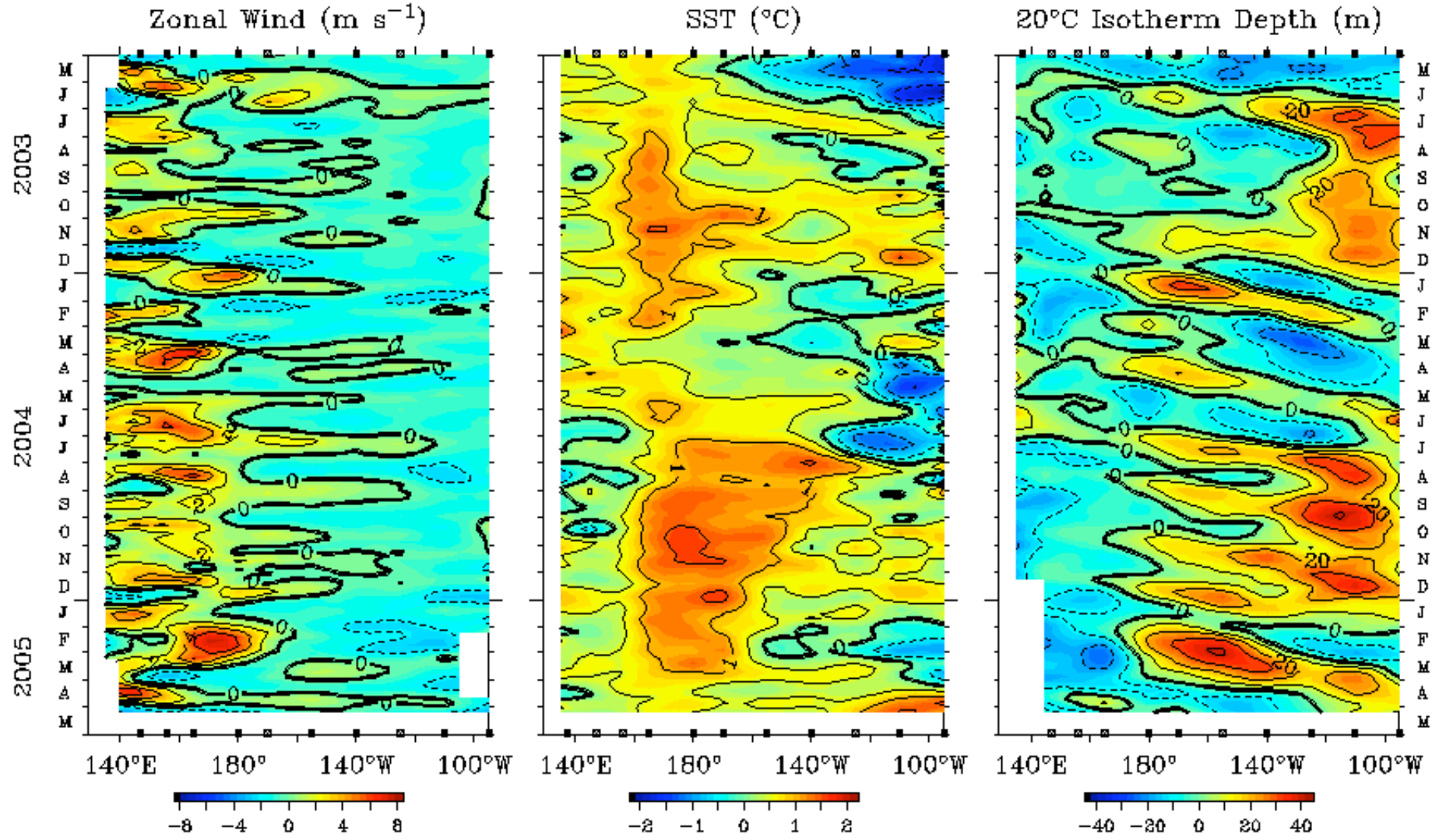

TAO Project Office/PMEL/NOAA

May 10 2005

Delayed Oscillator Theory

- Suarez and Schopf (1988); Schopf and Suarez(1988)
- Battisti (1988); Battisti and Hirst (1989)

- El Niño due to a ménagerie of oceanic Kelvin and Rossby modes

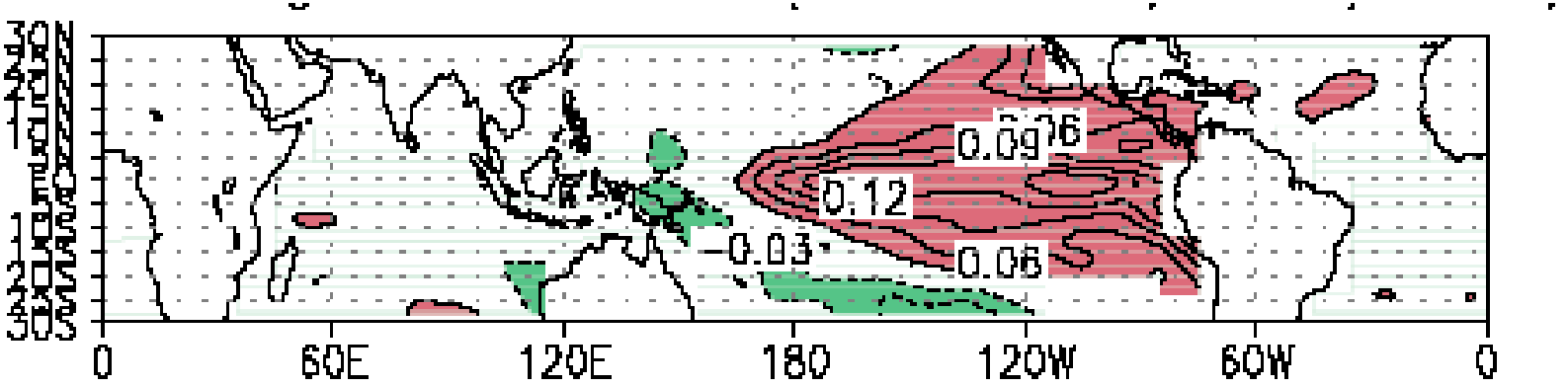

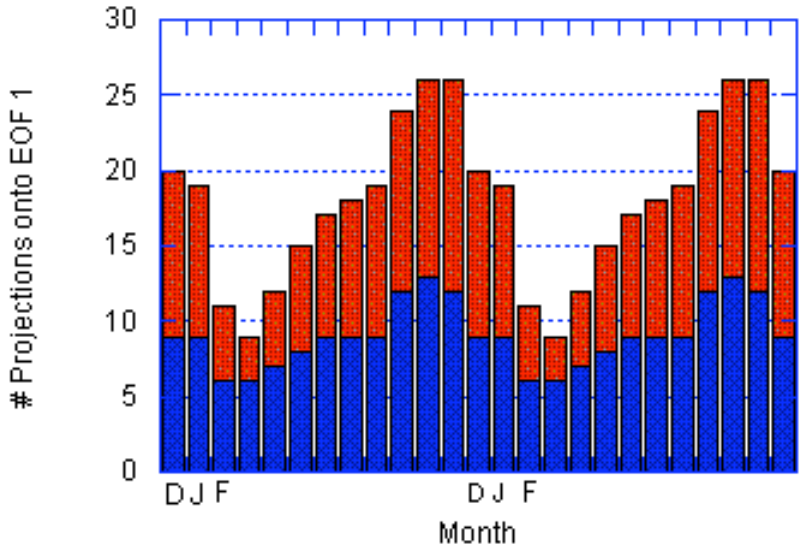

|pattern correlation| > 0.5

(~600 months of COADS data)

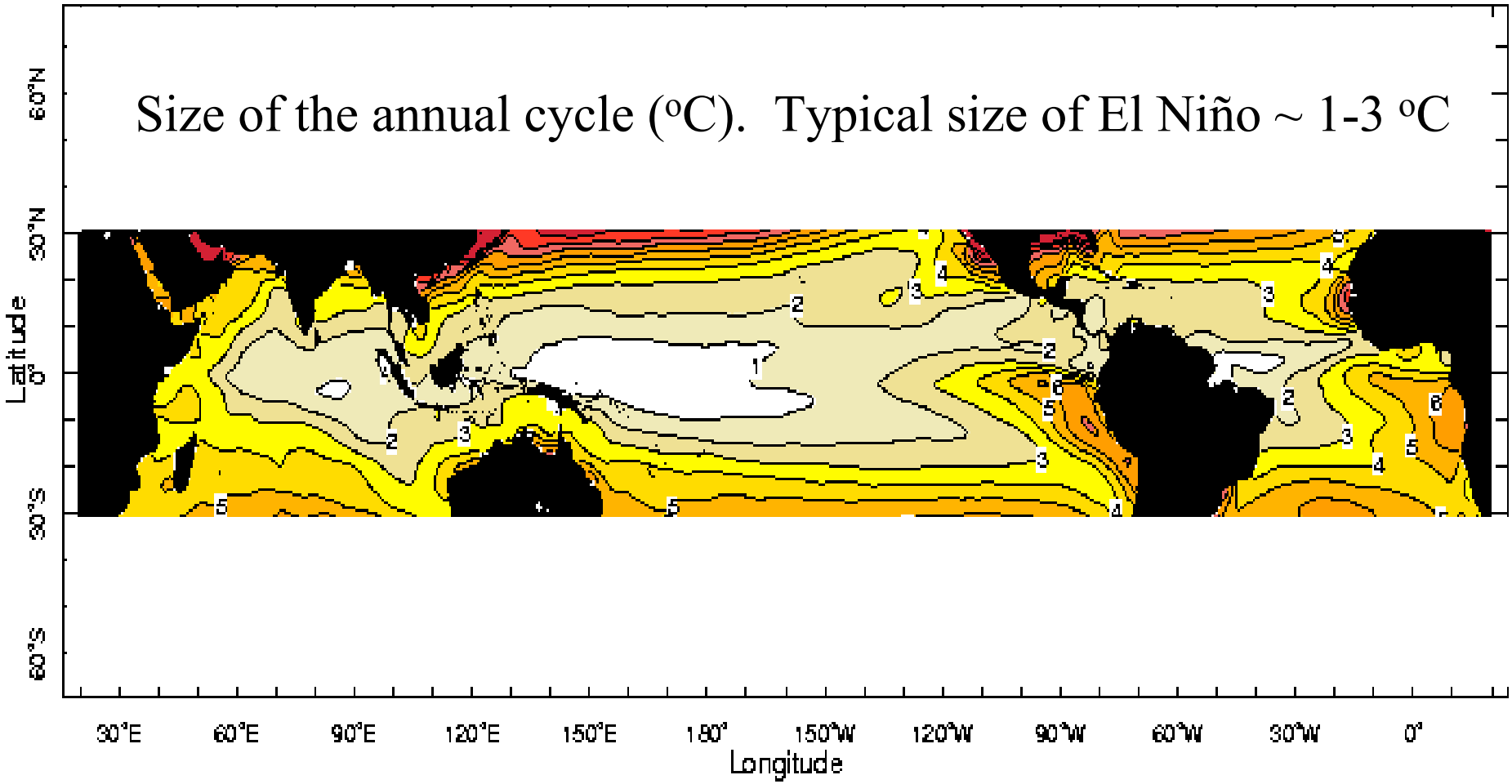
Size of the annual cycle (ºC). Typical size of El Niño ~ 1-3 ºC
60°N
30°N
0°
30°S
60°S
Latitude
30°E
60°E
90°E
120°E
150°E
180°
150°W
120°W
90°W
60°W
30°W
0°
Longitude

Linear Inverse Modeling

(Penland 1989; POP analysis: Hasselmann 1988, von Storch et al. 1988; Penland and Sardeshmukh 1995)

Using a two-parameter linearization, we obtain for SST anomalies around the annual cycle:

$$d\boldsymbol{T}/dt = \mathbf{B}\boldsymbol{T} + \boldsymbol{\xi}, \text{ with } \langle \boldsymbol{\xi}(t+\tau)\, \boldsymbol{\xi}^{\boldsymbol{T}}(t) \rangle = \mathbf{Q}(t)\delta(\tau)$$

For now, we'll assume $\boldsymbol{\xi}$ behaves as additive white noise, although that assumption is generally false. $\mathbf{Q}(t)$ is periodic.

Corresponding FPE:

$$\frac{\partial p(\boldsymbol{T},t)}{\partial t} = -\sum_{ij} \frac{\partial}{\partial T_i}\left[B_{ij} T_j\, p(\boldsymbol{T},t)\right] + \frac{1}{2}\sum_{ij} \frac{\partial^2}{\partial T_i \partial T_j}\left[Q_{ij}(t)\, p(\boldsymbol{T},t)\right]$$

From the FPE.

$p(\boldsymbol{T},t+\tau|\boldsymbol{T}_o,t)$ is Gaussian, centered on $\mathbf{G}(\tau)\,\boldsymbol{T}_o$

where $\mathbf{G}(\tau) = \exp(\mathbf{B}\tau) = <\boldsymbol{T}(t+\tau)\boldsymbol{T}^{\mathrm{T}}(t)><\boldsymbol{T}(t)\boldsymbol{T}^{\mathrm{T}}(t)>^{-1}$.

The covariance matrix of the predictions:

$$\boldsymbol{\Sigma}\,(t,\tau) = <\boldsymbol{T}(t+\tau)\boldsymbol{T}^{\mathrm{T}}(t+\tau)> - \mathbf{G}(\tau) < \boldsymbol{T}(t)\boldsymbol{T}^{\mathrm{T}}(t)> \mathbf{G}^{\mathrm{T}}\,(\tau)\ .$$

Further,

$$\frac{\partial}{\partial t} < \boldsymbol{T}(t)\boldsymbol{T}^{\mathrm{T}}(t)> = \mathbf{B} < \boldsymbol{T}(t)\boldsymbol{T}^{\mathrm{T}}(t)> + < \boldsymbol{T}(t)\boldsymbol{T}^{\mathrm{T}}(t)> \mathbf{B}^{\mathrm{T}} + \mathbf{Q}(t)$$

Digression #1: *The disturbing assumption of additive noise*.

Instead of $d\boldsymbol{T}/dt = \mathsf{B}\boldsymbol{T} + \boldsymbol{\xi}$, the system is actually of the form

$d\boldsymbol{T}/dt = \mathsf{B}\boldsymbol{T} + (\mathsf{A}\boldsymbol{T} + \mathsf{C})\boldsymbol{\xi}_1 + \mathsf{D}\boldsymbol{\xi}_2$.

All of the LIM formalism follows through, with the identification

$$\mathsf{B} \rightarrow \mathsf{B} + \mathsf{A}^2/2; \quad \mathsf{Q} \rightarrow \langle(\mathsf{A}\boldsymbol{T} + \mathsf{C})\,(\mathsf{A}\boldsymbol{T} + \mathsf{C})^{\mathrm{T}}\rangle + \mathsf{D}\mathsf{D}^{\mathrm{T}}$$

$$\mathsf{G}(\tau) \rightarrow exp\ \{\ (\mathsf{B} + \mathsf{A}^2/2)\,\tau\ \}$$

- Note: $p(\boldsymbol{T}, t+\tau \,|\, \boldsymbol{T}_o, t)$ is no longer Gaussian, but $\mathsf{G}(\tau)\,\boldsymbol{T}_o$ is still the best prediction in the mean square sense.

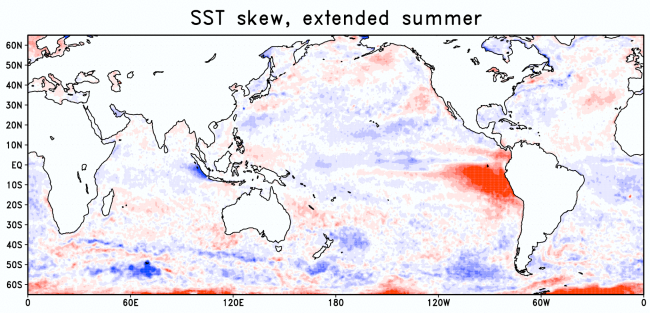

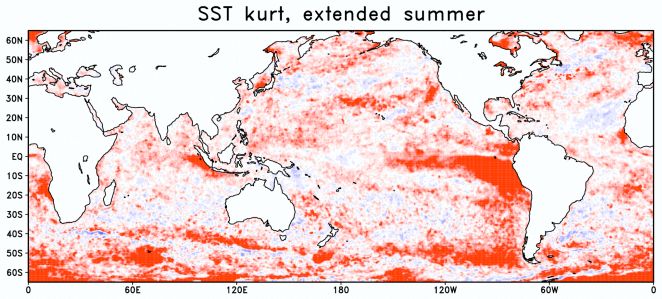

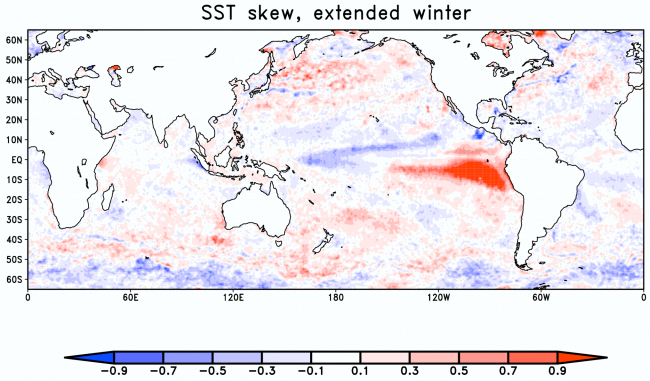

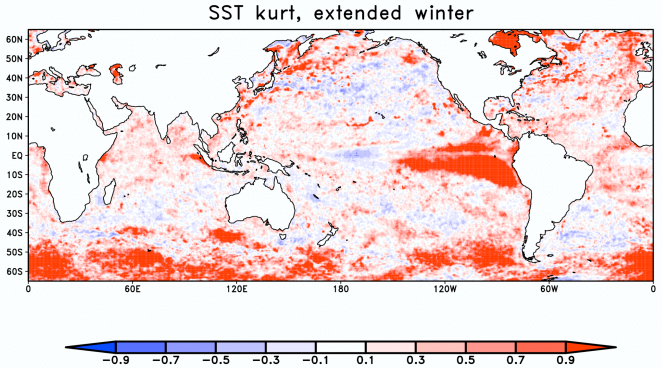

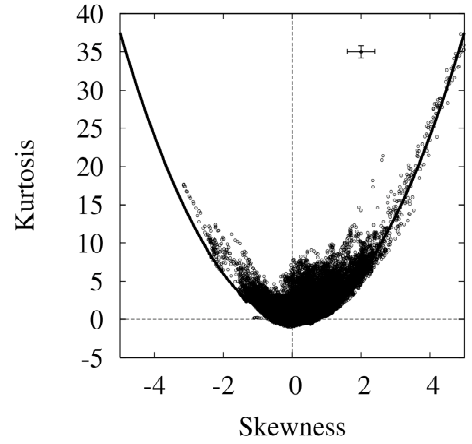

Sura and Sardeshmukh 2007

Eigenvectors of $\mathbf{G}(\tau)$ are the ***"normal" modes*** $\{\mathbf{u}_i\}$.

Eigenvectors of $\mathbf{G}^{\mathrm{T}}(\tau)$ are the ***"adjoints"*** $\{\mathbf{v}_i\}$,

(Recall: $\mathbf{G}(\tau) = \langle \boldsymbol{T}(t+\tau)\boldsymbol{T}^{\mathrm{T}}(t) \rangle \langle \boldsymbol{T}(t)\boldsymbol{T}^{\mathrm{T}}(t) \rangle^{-1}$)

and $\mathbf{u}\mathbf{v}^{\mathrm{T}} = \mathbf{u}^{\mathrm{T}}\mathbf{v} = \boldsymbol{1}$.

Most probable prediction: $\boldsymbol{T}(t+\tau) = \mathbf{G}(\tau)\ \boldsymbol{T}_o\ (t)$

The neat thing: $\mathbf{G}(\tau) = \{\mathbf{G}(\tau_o)\}^{\tau/\tau_o}$.

If LIM's assumptions are valid, the prediction error $\boldsymbol{\varepsilon} = \boldsymbol{T}(t+\tau) - \mathbf{G}(\tau)\ \boldsymbol{T}_o$ does not depend on the lag at which the covariance matrices are evaluated. This is true for El Niño; it is *not* true for the chaotic Lorenz system.

Below, different colors correspond to different lags used to identify the parameters. What is plotted: $Tr(\Sigma)$ *vs* lead.

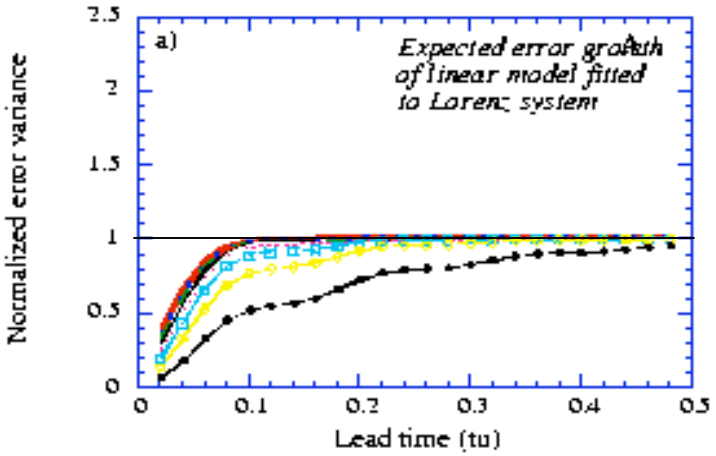

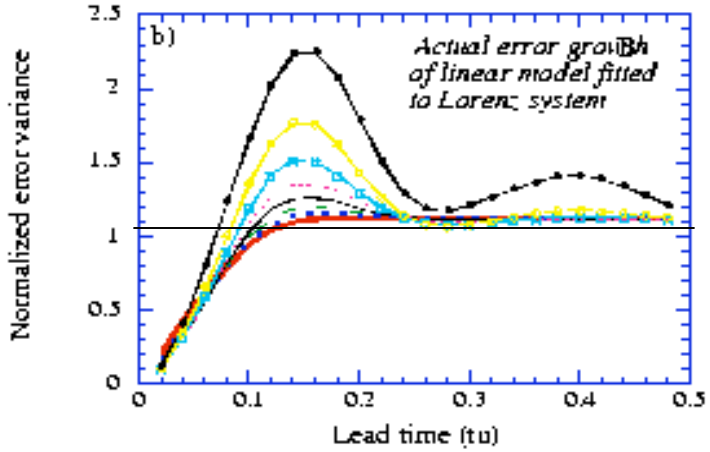

Penland and Sardeshmukh (1995)

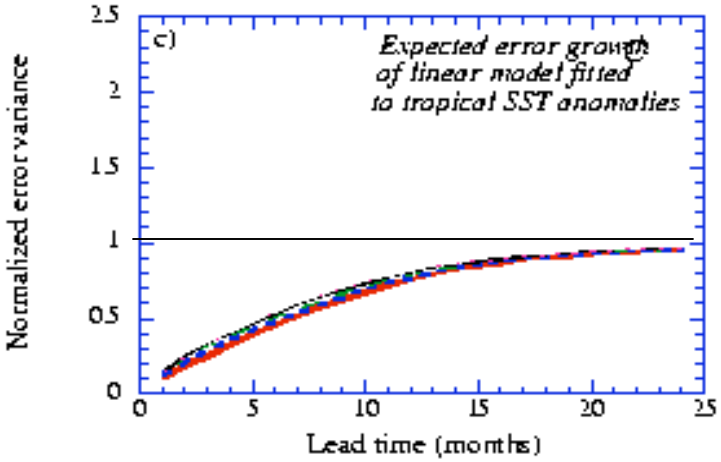

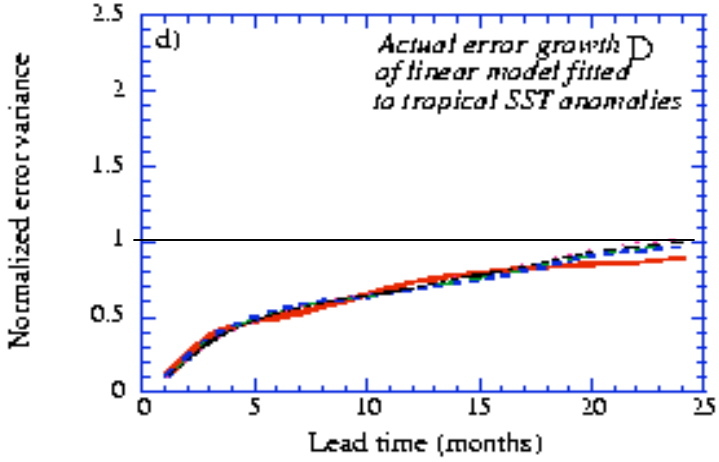

A model generated with the stationary **B** *and* the stochastic forcing with cyclic statistics **Q**(*t*) *does* reproduce the correct phase-locking of El Niño/ La Niña with the annual cycle.

(Note: Generate model using Kloeden and Platen (1992))

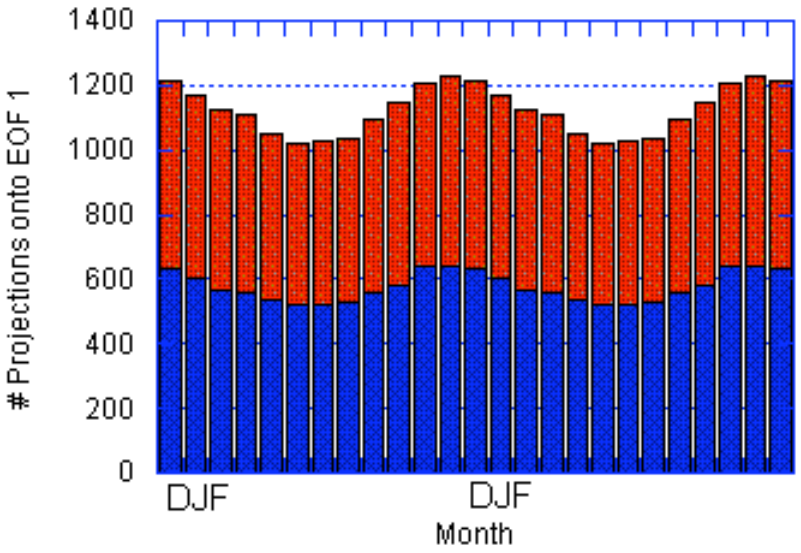

|pattern correlation| > 0.5

(~24 000 months of model data)

When a system is linear, we can completely identify it from data (***Linear Inverse Modeling***). When it is multi-dimensional, its size can temporarily *grow*, even though all of its components are *decaying*. This happens if the components are almost never orthogonal.

Farrell (1988)

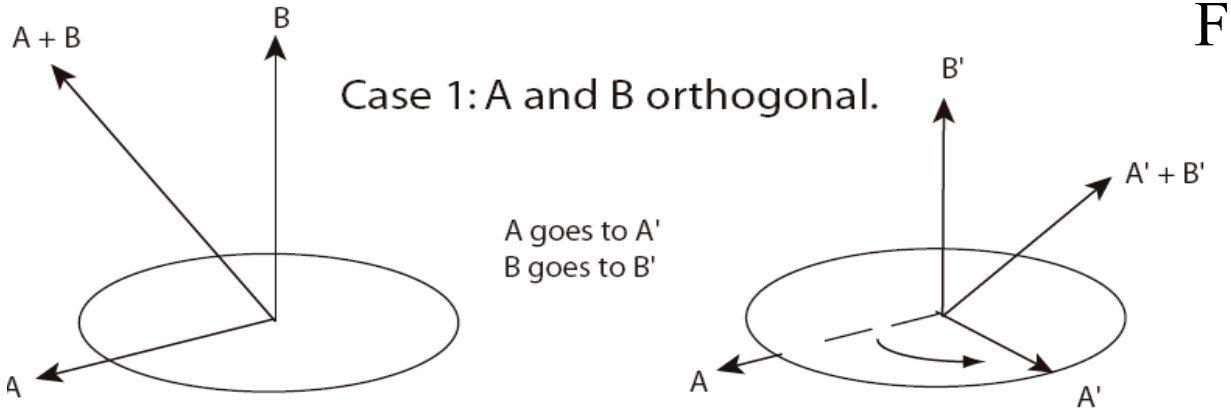

(A' + B') is shorter than (A + B)

B and C are the same length.
B' and C' are the same length.

Case 2: A and C non-orthogonal.

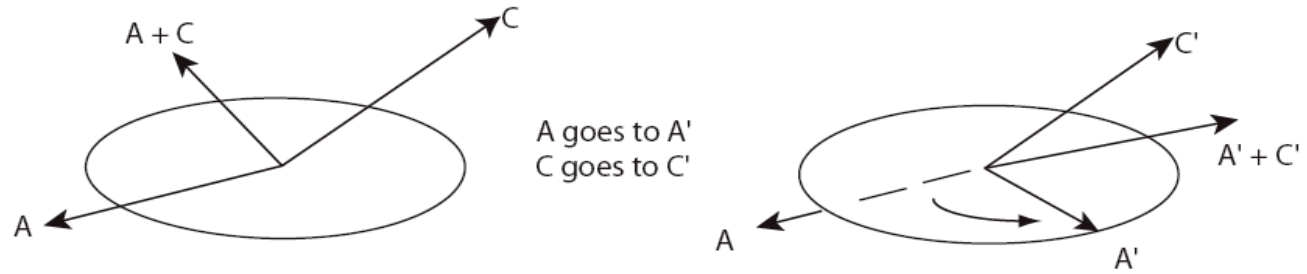

(A' + C') is longer than (A + C)

Optimal initial structure for growth over lead time τ:

Right singular vector of $\mathbf{G}(\tau)$ (eigenvector of $\mathbf{G}^T\mathbf{G}(\tau)$)

Growth factor over lead time τ:

Eigenvalue γ of $\mathbf{G}^T\mathbf{G}(\tau)$. (Penland and Sardeshmukh 1995)

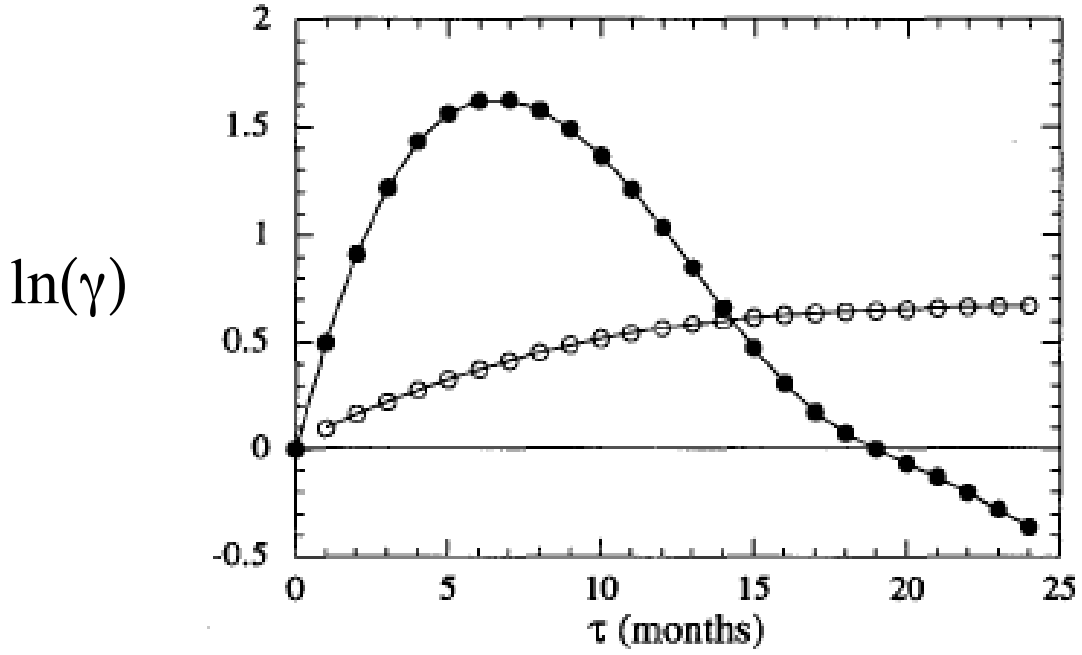

The transient growth possible in a multidimensional linear system occurs when an El Niño develops. ***LIM*** predicts that an *optimal pattern* (*a*) precedes a mature El Niño pattern (*b*) by 6 to 8 months

a)

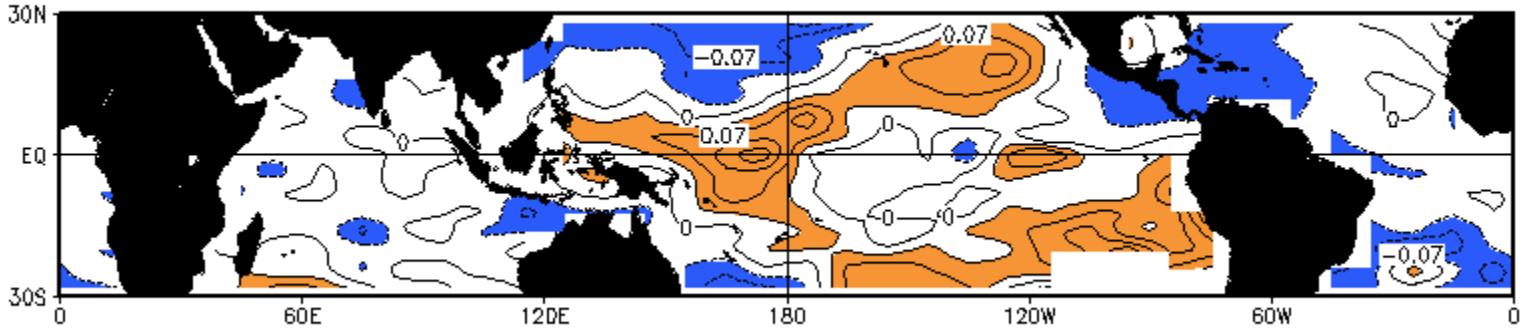

b)

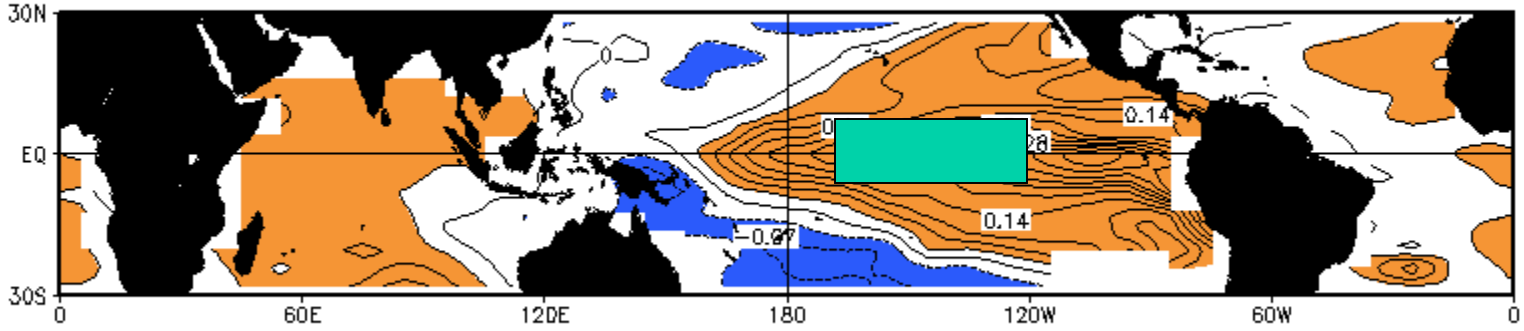

Temp. Anom. in Niño 3.4 region (6°N-6°S, 170°W-120°W): $\delta T_{3.4}$

This time series virtually identical with *PC 1*.

c)

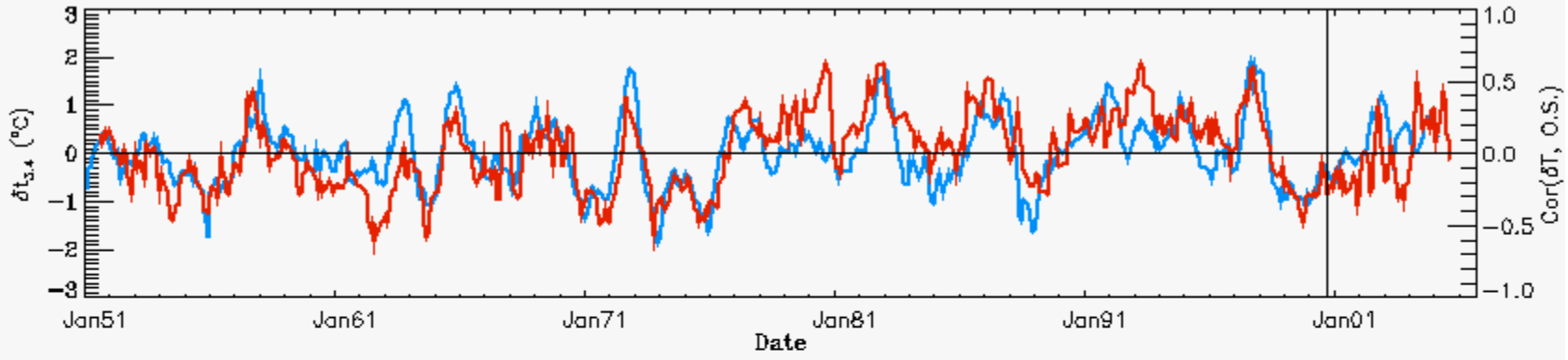
3
2
1
0
−1
−2
−3
δt3.4 (°C)
1.0
0.5
0.0
−0.5
−1.0
Cor(δT, O.S.)
Jan51
Jan61
Jan71
Jan81
Jan91
Jan01
Date

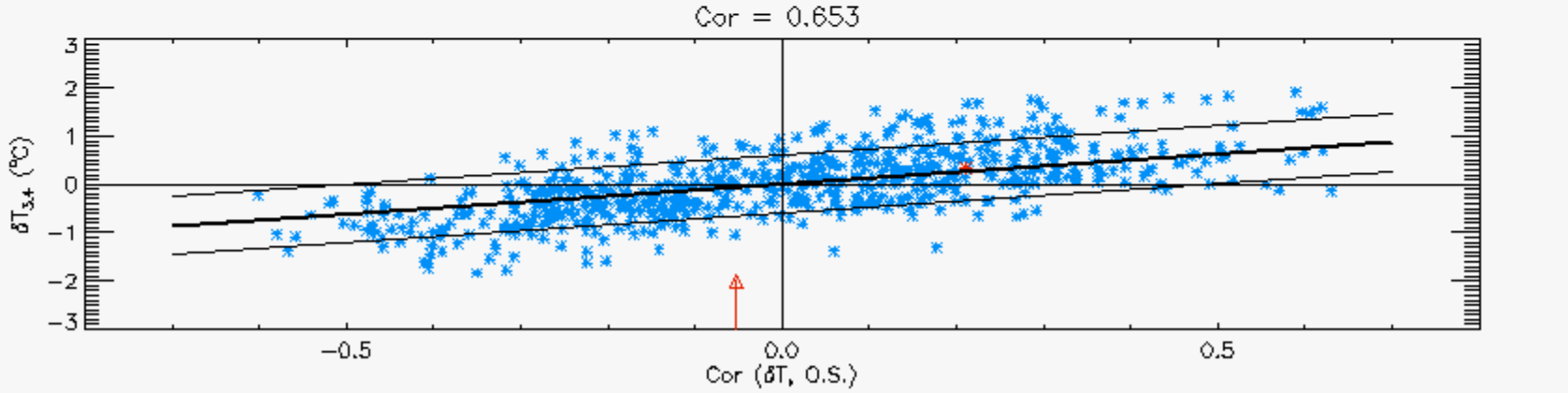
Cor = 0.653
3
2
1
0
−1
−2
−3
δT3.4 (°C)
−0.5
0.0
0.5
Cor (δT, O.S.)

But where does the optimal structure come from? Recall that this pattern is a statistical compromise of ALL sensitive regions.

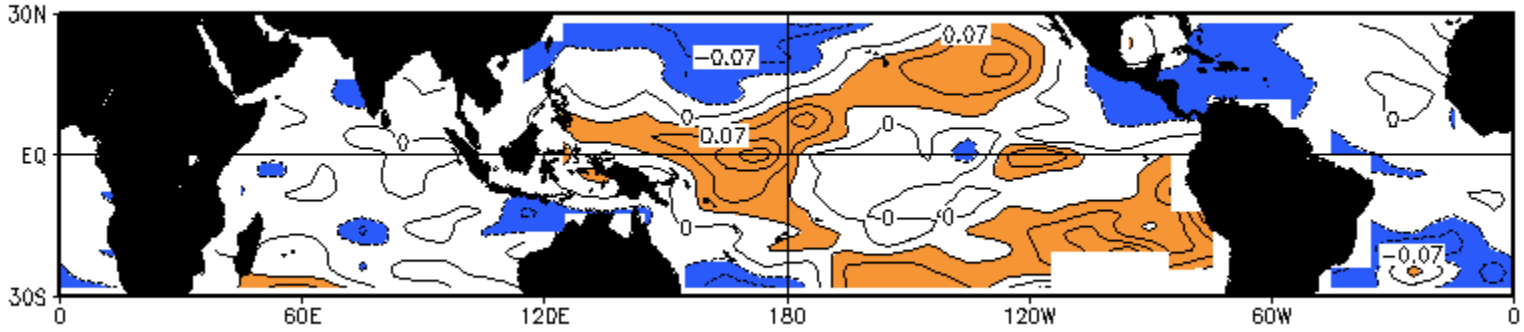

- Oceanic Kelvin waves generated by westerly wind bursts over the Maritime continent (McPhaden, Kleeman, Kessler, etc.)
- Temperature advection by instability waves (e.g., Legeckis; Jochum and Murtugudde)
- "Seasonal footprinting mechanism" (Vimont et al 2003.)

Moore and Kleeman 1999

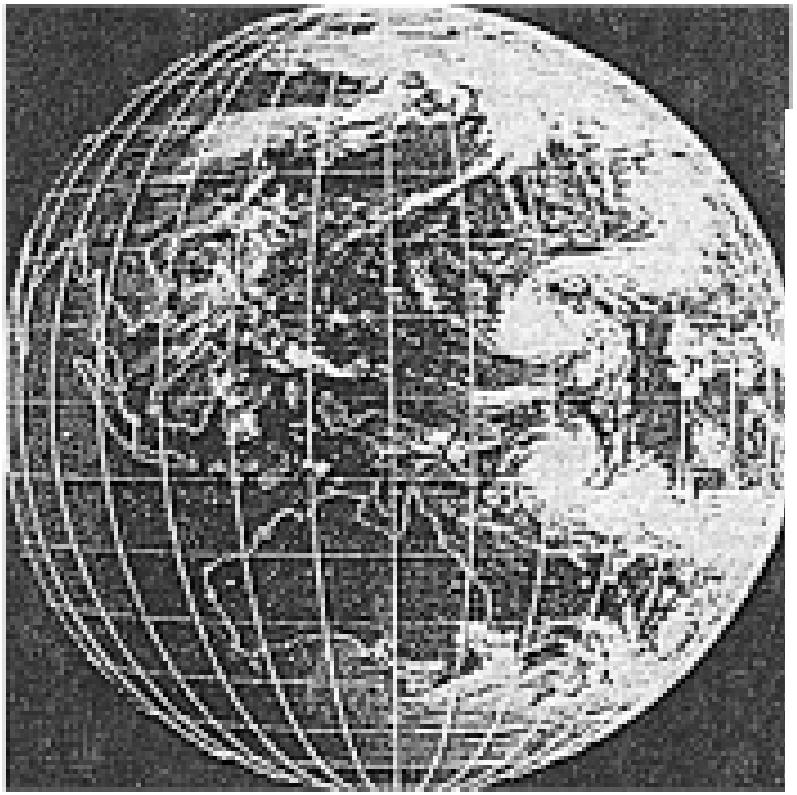

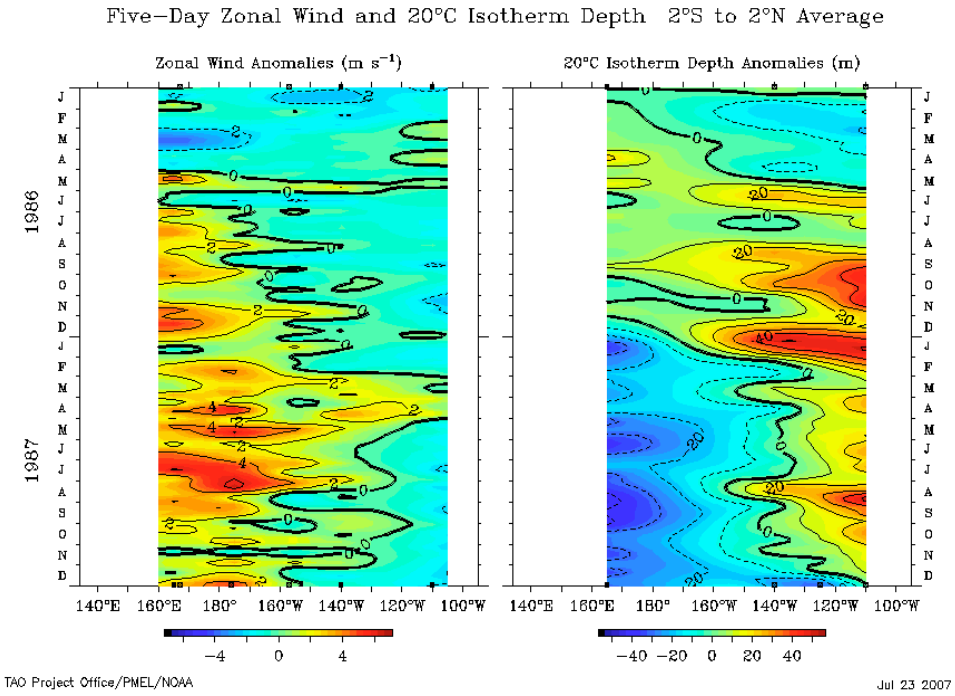

A satellite image from May 1986 showing the cloud formations associated with intense westerly wind burst activity and a pair of tropical cyclones (courtesy of the Taiwan Weather Bureau).

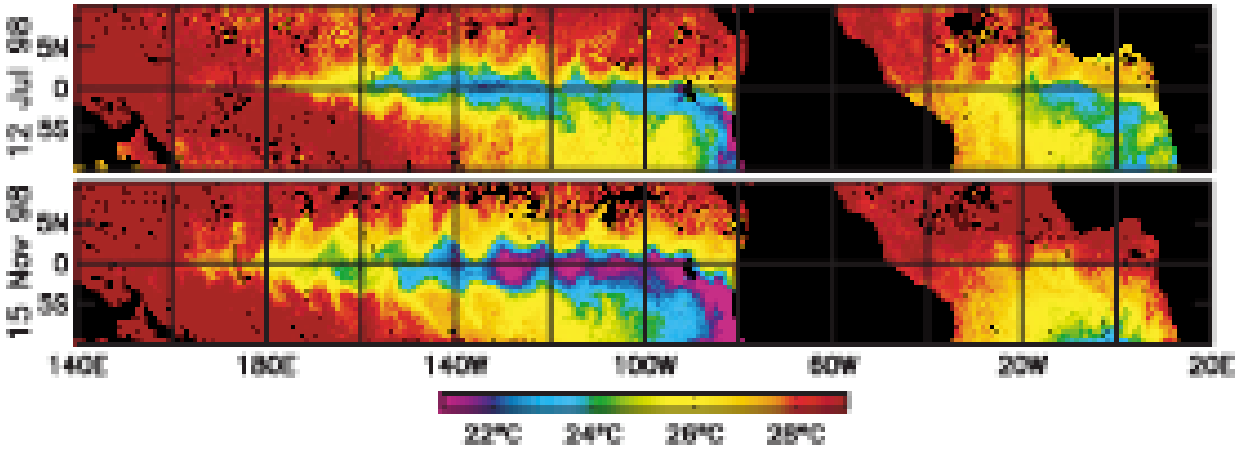

Plate 2. Selected 3-day composite-average maps of SST measured from the TMI for the periods 11-13 July 1998 (upper) and 14-16 November 1998 (lower). Black areas represent land or rain contamination.

D.B. Chelton, F.J. Wentz, Chelle L. Gentemann, R.A. deSzoeke, and M.G. Shlax. GRL, 27(9):1239-1242, 2000

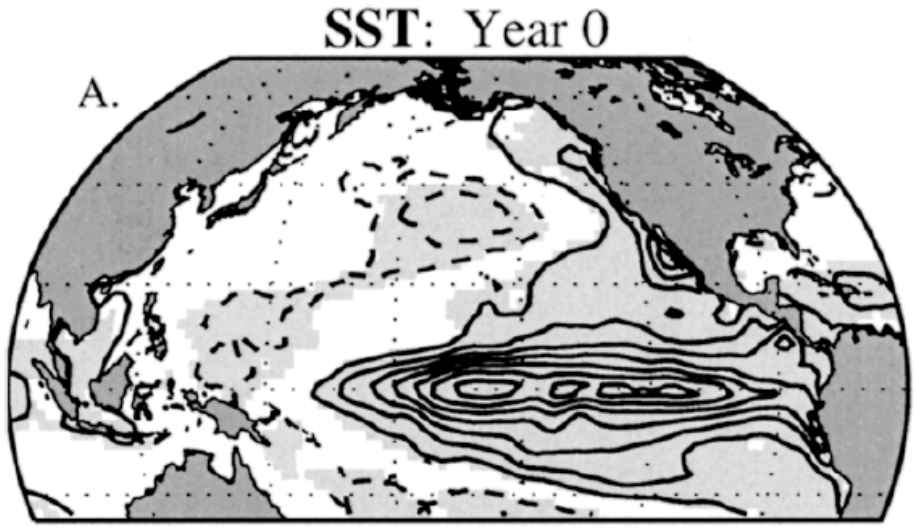

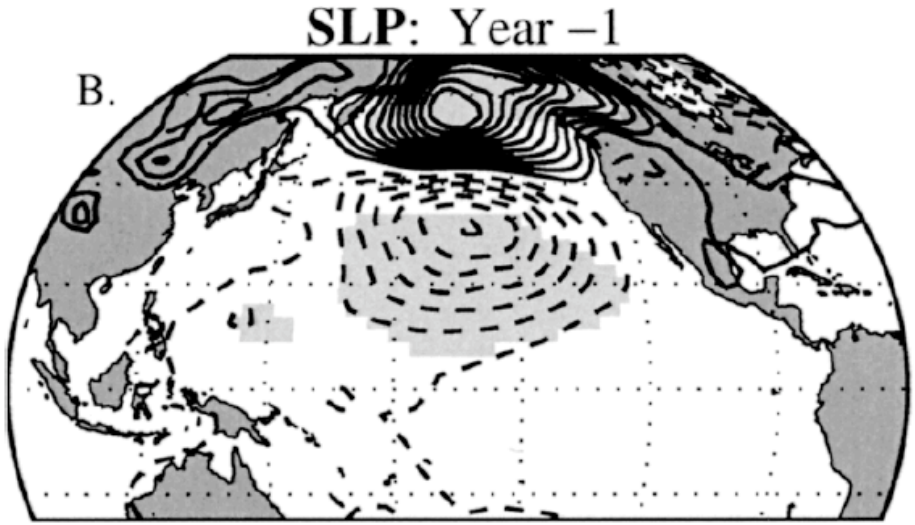

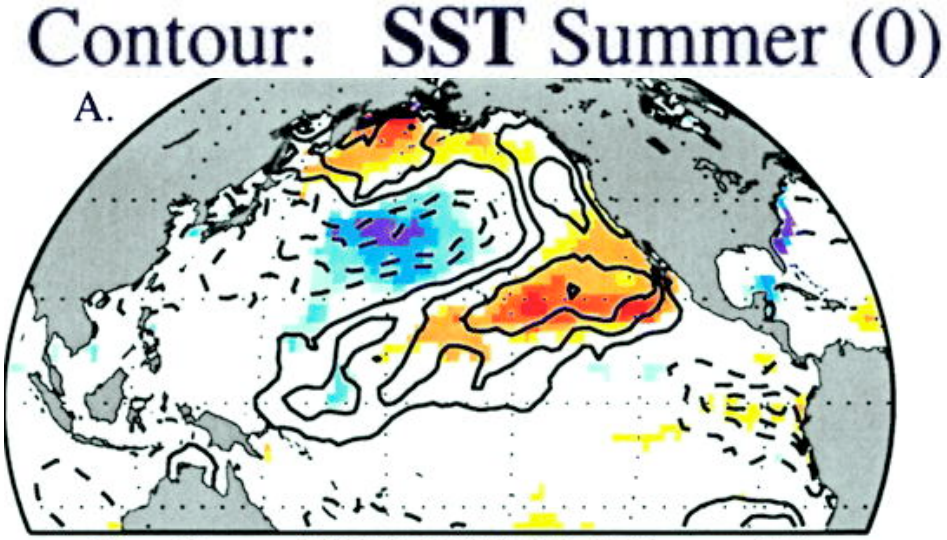

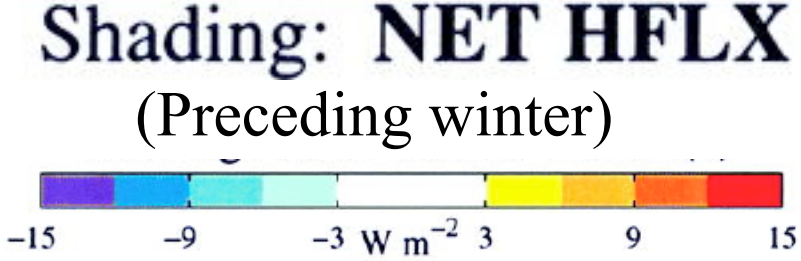

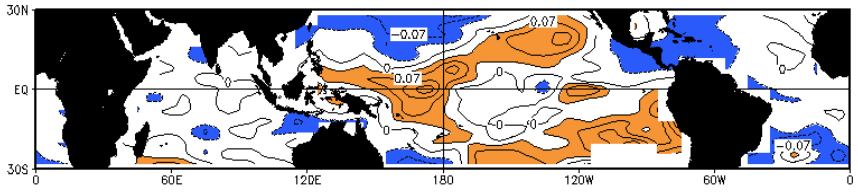

Vimont et al. 2003

Zhang et al. (1997)

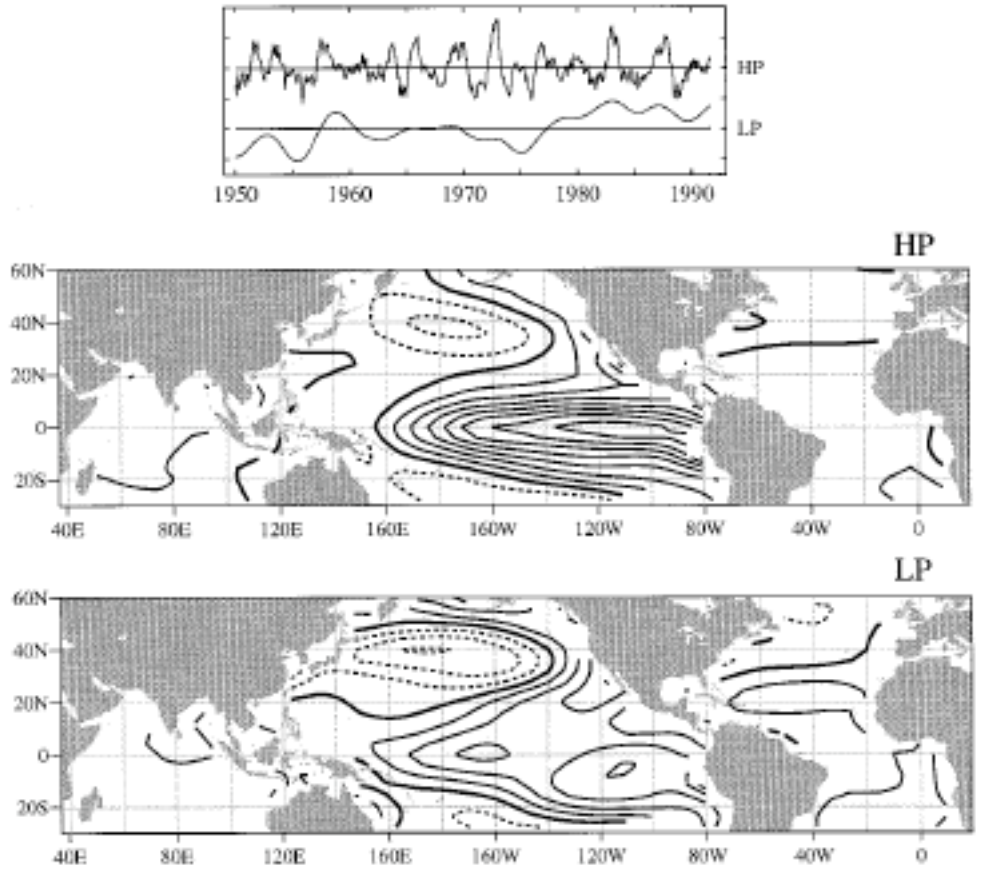

FIG. 3. The leading (normalized) PCs of 6-yr highpass- (HP) and lowpass- (LP) filtered SST over the Pacific domain shown together with the associated regression patterns for global SST. The interval between tick-marks on the vertical axis of the top panel corresponds to 1.0 standard deviation, and the spacing between the curves is arbitrary. Contour interval 0.1 K per standard deviation of the expansion coefficient time series. Negative contours are dashed; the zero contour is thickened.

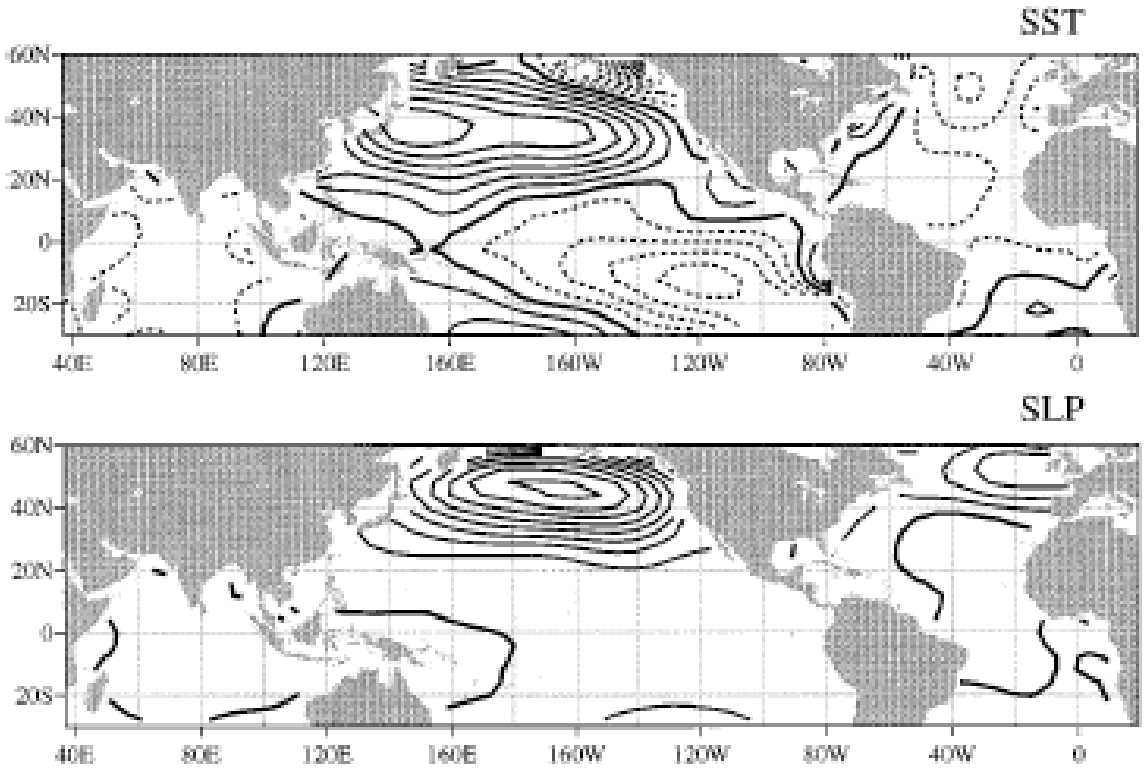

FIG. 15. Difference between time means: the epoch 1943–76 minus the previous epoch 1925–42. (top) The SST anomaly deviation field: contour interval 0.1 K. (bottom) The SLP field: contour interval 0.2 mb.

Alexander et al. (in press)

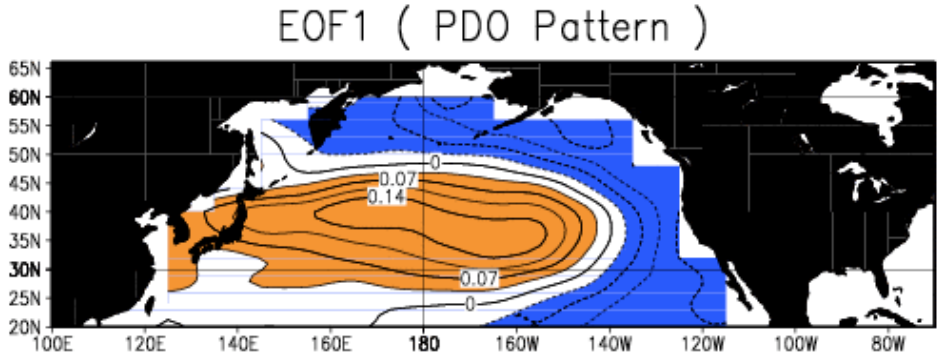

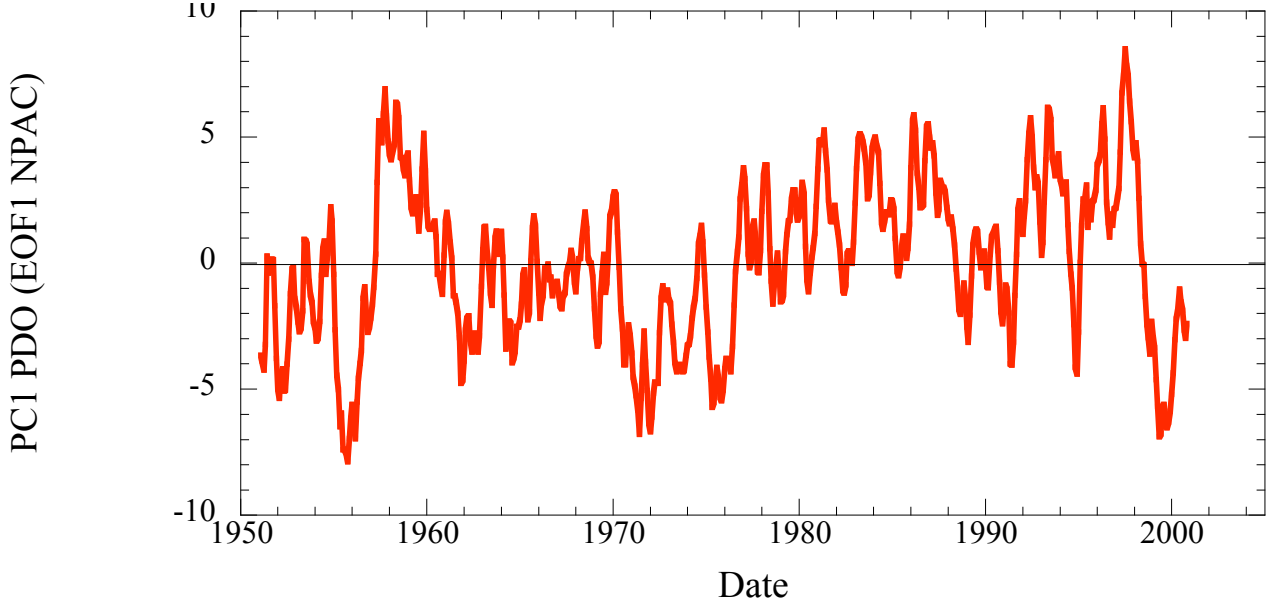

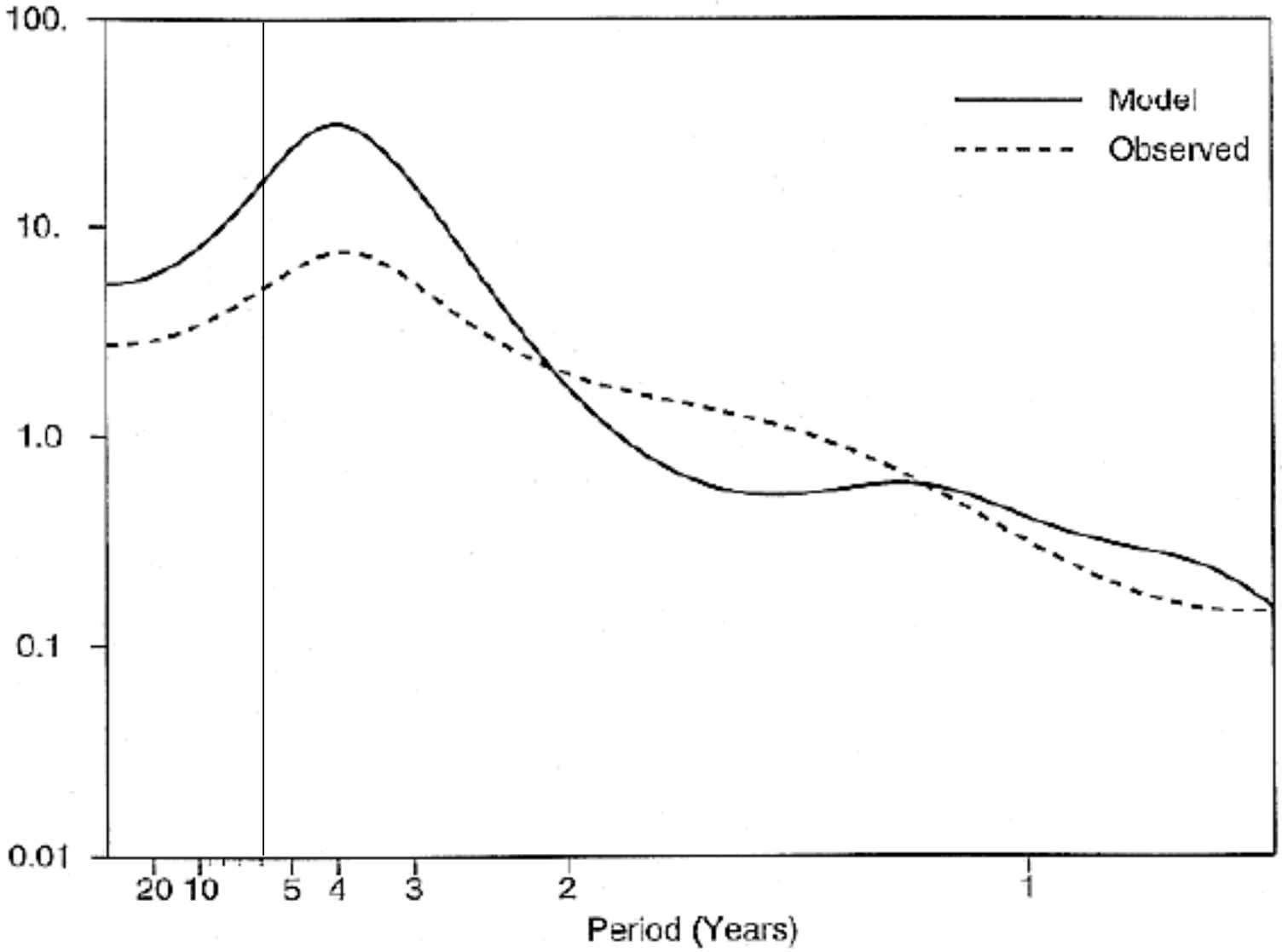

Fig. 3. A comparison of the power spectrum of the NINO3 index from the stochastically forced coupled model and observation. The spectra were computed using a maximum entropy method of order 30.

Moore and Kleeman (1999)

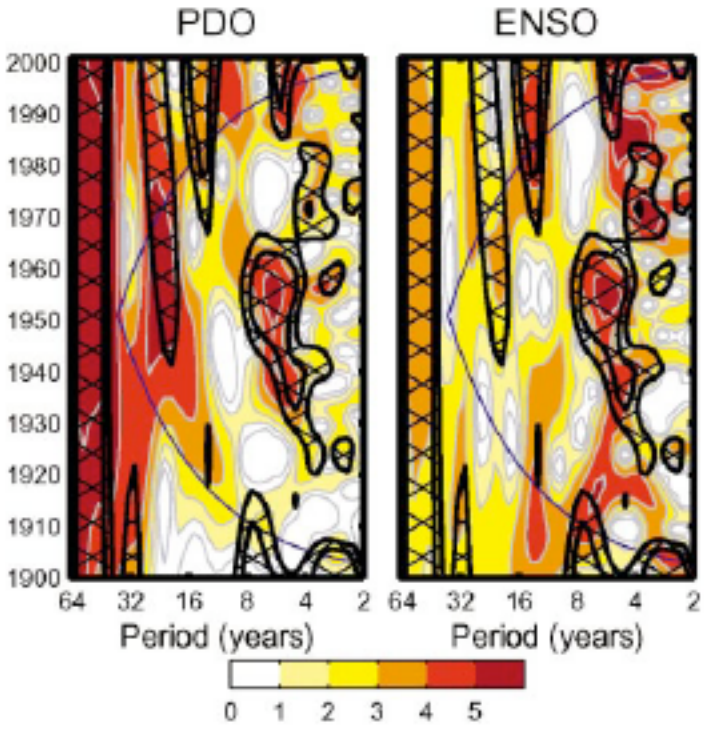

FIG. 2. Wavelet power spectrum of (left) PDO and (right) ENSO indices. Shading corresponds to $\log_2$(power); contours for values less than zero are omitted for clarity. The blue line indicates the cone of influence. Wavelet squared coherence exceeding 0.75 is indicated with the black contours (0.75 and 0.9) and hatching. Within the cone of influence, coherence of 0.76 (0.81) is 90% (95%) significant, based on a Monte Carlo simulation between 1000 sets (two each) of white noise time series.

Newman et al. (2003)

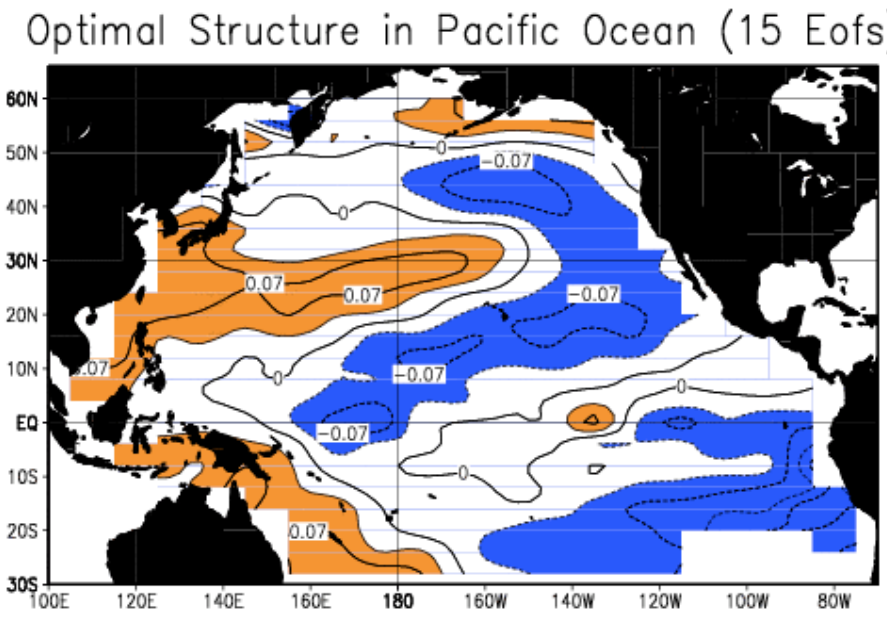

SST

Alexander et al. (in press)

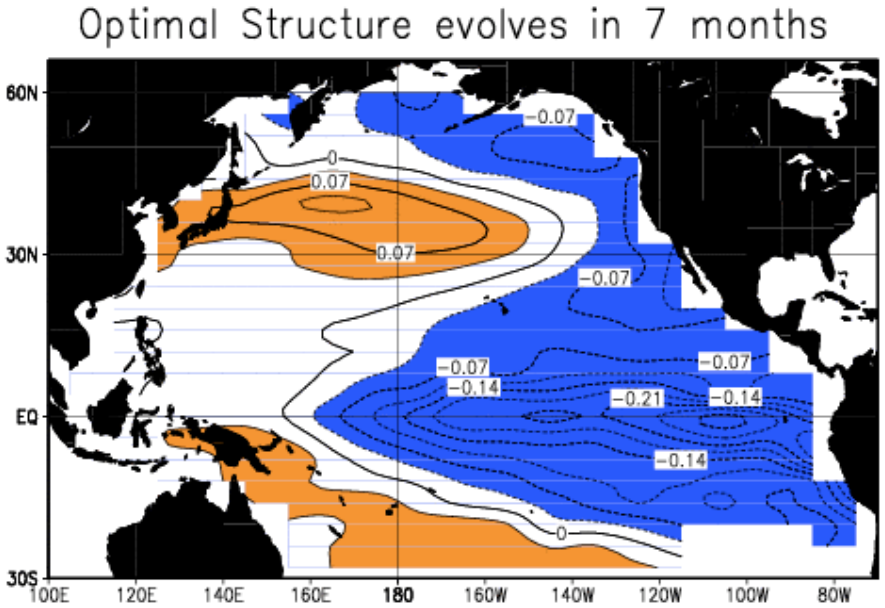

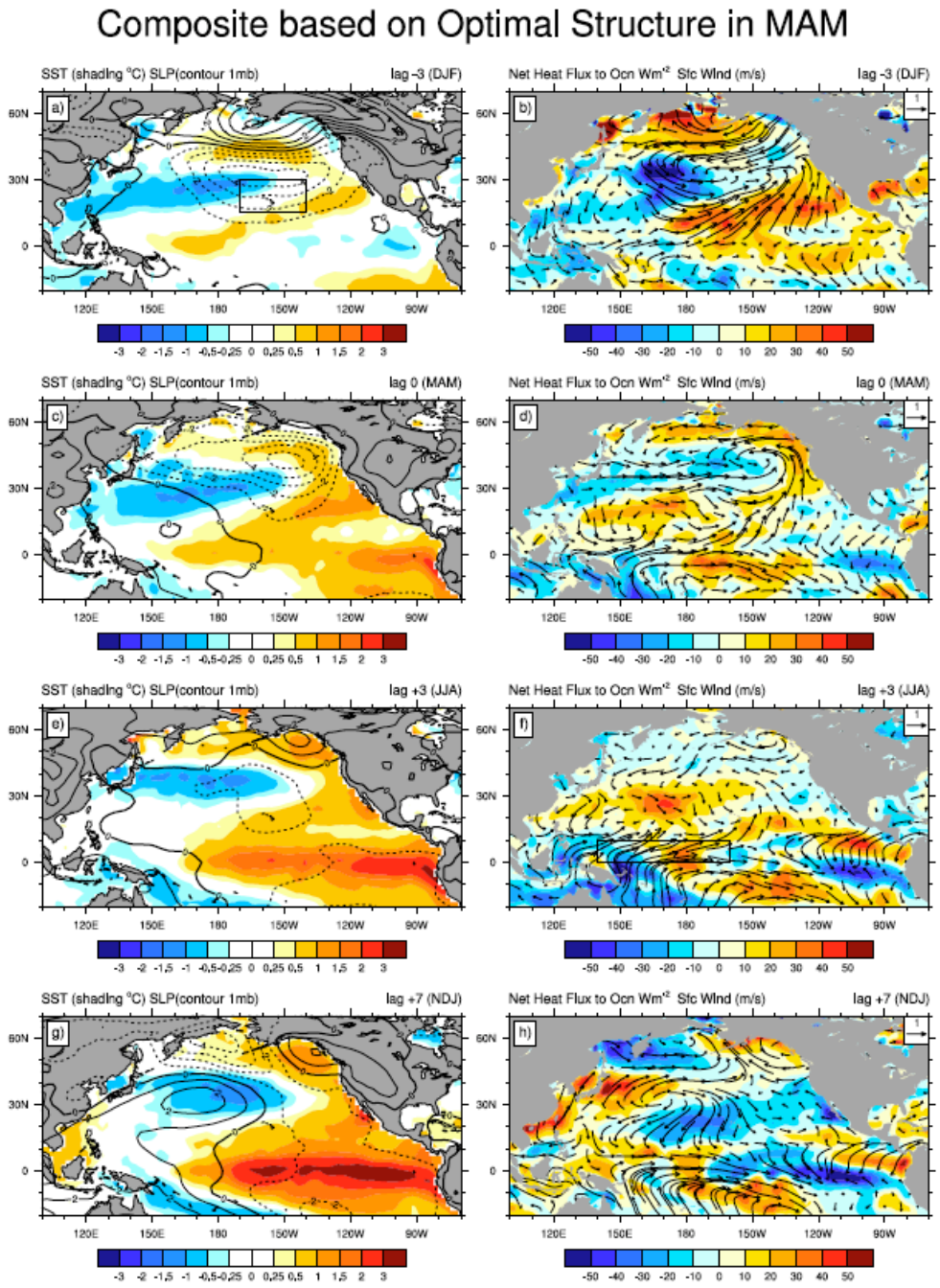

Alexander et al. (in press)

Conclusions

- El Niño is complicated.

- It's *so* complicated that it's basically linear and stochastic (> seasonal timescales)
- It's *not* so complicated that there isn't some limited predictability (τ up to about 1 year).
- Timescales related to El Niño range from hours (convection) to decades (PDO).

- A decade isn't as long as it used to be.

Shameless plug for my next talk

- How global a phenomenon *is* El Niño?
- Haven't we mostly ignored the Southern Hemisphere?